Case Studies in Thermal Engineering 70 (2025) 106080

Contents lists available at ScienceDirect

Case Studies in Thermal Engineering

journal homepage: www.elsevier.com/locate/csite

Design an asymmetrical 49-level inverter fed by battery and PV energy sources

Reving Masoud Abdulhakeem [a,c,*], Ali Kircay [a], Rakan Khalil Antar [b]

[a] Electrical and Electronics Engineering, Harran University, Sanliurfa 63000, Turkey
[b] Technical Engineering College, Northern Technical University, Mosul 41001, Iraq
[c] Computer Science Department, Nawroz University, Duhok 42001, Iraq

ARTICLE INFO

Keywords:
Multilevel inverter
Asymmetrical topology
THD
Renewable energy integration
Photovoltaic systems
Power quality

ABSTRACT

This study investigates the design and performance of an asymmetrical 49-level cascaded inverter specifically developed for renewable energy applications. The inverter's operation is analyzed under three distinct scenarios: utilizing DC battery sources configured in a per-unit voltage ratio (1:2:7:14), employing DC batteries with actual voltage levels (40:80:280:560 V), and replacing the DC sources with photovoltaic (PV) modules. The simulation results demonstrate the inverter's exceptional capability to produce high-quality sinusoidal output voltage and current waveforms with significantly low harmonic distortion. In the per-unit voltage configuration, the inverter achieves an RMS voltage (Vo_{RMS}) of 16.9719V and an RMS current (Io_{RMS}) of 1.0569A, with a total harmonic distortion of 0.71216 % for voltage (THD_{Vo}) and 0.093319 % for current (THD_{Io}). When configured with actual voltage levels, the system delivers Vo_{RMS} = 679.0492V and Io_{RMS} = 4.265A, with THD_{Vo} of 0.71227 % and THD_{Io} of 0.16719 %. With PV modules system, the inverter achieves Vo_{RMS} = 692.7293V and Io_{RMS} = 43.1367A, and the THD values for output voltage and current were 1.2926 % and 0.33963 %, respectively. These results highlight the inverter's versatility and efficiency in providing high-quality power output while maintaining minimal harmonic distortion, making it a promising solution for modern renewable energy systems and industrial applications.

1. Introduction

The Multilevel inverters have now made a strong entry into the contemporary power systems as one of the most significant enablers of power quality improvement and efficient energy control in renewable energy and smart grid technologies. Compared to conventional inverters, multilevel inverters have their advantages in terms of lower total harmonic distortion, and better system efficiency, which make them crucial for PV system and energy storage system. One of the main research interests is the use of energy storage systems synchronized with multilevel inverters in microgrid to enhance the energy distribution and the efficiency of storage systems [1]. In this regard, integration of the two structures guarantees compatibility with smart grid technologies for efficient energy management and load balancing.

Multilevel topologies are inevitable in high-performance applications and the optimization technique aims to improve the performance of multilevel inverters specifically in PV integrated systems. Scientific approaches, including incorporation of enhanced control structures and search algorithms, have been utilized to enhance power quality (PQ) [2,3]. For example, papers on the extent of third-order sliding mode controllers in optimizing the grid power quality in PV systems using different optimization strategies [4].

* Corresponding author. Electrical and Electronics Engineering, Harran University, Sanliurfa 63000, Turkey.
E-mail address: revinkmasoud@gmail.com (R.M. Abdulhakeem).

https://doi.org/10.1016/j.csite.2025.106080
Received 16 December 2024; Received in revised form 10 March 2025; Accepted 1 April 2025
Available online 2 April 2025

Utility systems employing multilevel inverters can be facilitated by superior control schemes for accomplishing different goals such as total harmonic distortion (THD_ mitigation. These problems have been solved by adopting multi-objective techniques like the least squares pulse width modulation (LS-PWM) [5]. In the same way, highly reliable fault-tolerant control strategies are required for the effective operation and protection of microgrids with quasi-Z-source cascaded H-bridge multilevel inverters [6]. There has also been very much development in design and control structures of multilevel inverter circuits beside topologies. New structures like the switched-capacitor-based and flying-capacitor inverters help in reducing the number of devices needed and improving the power smoothing effect [7,8]. Furthermore, connected hybrid inverter topologies together with advanced energy storage systems also pose the prospect to enhance system solidity and power quality in renewable energies systems [9]. As multilevel inverter (MLI) is developing further, its means for the integration of PV systems into the grid enhances significantly. Sophisticated models and control techniques, including those with neutral point clamped inverters, have provided a solid foundation for managing the power flow in grid integrated system [10,11]. In addition, new approaches towards providing fault tolerance and energy smoothing are now in development for improved renewable energy systems [12,13].

Later developments have also proposed different configurations and control approaches in order to gain the highest performance depending on the conditions in the grid. For example, with regard to control strategies for neutral point clamped inverters, the examined modeling shows potential for smooth connection of three-phase PV systems to the grid. These configurations lead to improved mechanisms for harmonic suppression and enhanced system reliability, which are crucial in dynamic energy conditions [14]. Further, the topologies for PV systems implemented in quasi-Z-source cascaded H-bridge multilevel inverter grid have an improved stability and power supply, which are important in microgrid systems [15].

In summary, multilevel inverters are emerging as perhaps the most vital invention in today's electric power systems with extensive research effort being devoted to their application, integration as well as advanced control schemes for efficient utilization in renewable energy systems.

2. Literature review

Multilevel inverters are known to have major duties of improving power quality and incorporating renewable energy resources into the grid. Many topologies, control techniques, and optimization methods have been proposed for enhancing their operation in different applications. The model predictive control has been implemented to control microgrids integrated with energy storage and PV systems in quasi-Z-source cascaded H-bridge multilevel inverters to achieve better dynamic response and fault tolerance [16]. Likewise, better control approaches for a 15-level modified cascaded H-bridge inverter in combination with PV and energy storage systems have been proved satisfactory in controlling energy distribution and minimizing harmonic [17]. In standalone PV systems, new multifunctional inverter structures joined with varying control algorithms have produced some advancement in comparatively low THD and/or converter efficacy [18]. Furthermore, improved control methods for single-phase multilevel cascaded converters applied to distributed PV and battery energy storage systems have been established for enhanced energy distribution and system dependability [19]. Controlled device count configurations are being considered for their low cost and simplicity in renewable energy systems. For instance, single phase multilevel inverters employing multicarrier pulse width modulation (MCPWM) technique for better performance for solar system have been developed [20]. Asymmetric cascaded E-type multilevel inverters have also been used to advance fault ride-through capability of wind turbine systems by integrating dynamic voltage restorers with them [21]. The multilevel inverter structures have also been discussed to be modified for their applicability in the PV system. Out of these configurations, research on these structures show that they have the potential to exhibit higher efficiency and lower switching losses, thus suitable for both grids interfaced and off-grid application [22]. Incorporation of hybrid filters along with multilevel inverters has also improved the power quality of the utility network even more efficiently, using spotted hyena optimized algorithms for optimizing the harmonic current in the context of PV systems [23]. Recent comparative analysis of transformerless MLIs control and configurations with different modulation techniques found research works that show compromise solution of regarding efficiency, cost and implement ability in renewable energy systems [24]. Model predictive control has also been used in nine-level inverters where performance of renewable energy systems has been optimized through effective power integration and dynamic stability [25]. New topologies of reduced-switch multilevel inverters for grid-connected photovoltaic systems have proposed for efficient integration of the renewable energy source and for improved power control [26]. Today, incorporation of multilevel unified power flow controllers for grid integration of solar photovoltaic systems and several other feeders has enhanced proven reliability and stability through multiple advanced optimization techniques [27]. Furthermore, enhancing the power quality of renewable energy sources through an integration of seven-level converter, controlled by novel methodologies has verified that green energy systems are capable of operating at high levels of efficiency and flexibility while optimizing their interfaces to other circuits [28]. Modular multilevel inverter structures have also enhanced power quality green building microgrids and energy efficiency in sustainable structure [29]. Successful strategies of grid-connected power injection have been established in hybrid renewable energy systems which comprises multilevel inverters to increased power and performance from both solar and wind energy [30]. Furthermore, coordinated control at the multilevel has enabled integration of electric vehicle charging stations with islanded DC microgrid faced challenges in fault ride through capability and dynamic energy management [31]. Current research in multilevel inverter circuit basically discusses new methods of control structures which allow more variation in handling of the various topologies of inverter circuits involving or not involving three phase inverters. It was observed that these designs focus on efficient integration of renewable power supply and enhance the system control [32]. Further, the enhancement of renewable power energy management stresses simple inverter designs that may vary depending on the type of system single-phase or three-phase as well as affect acute power fine distribution and system steadiness in various renewable energy predicaments [33]. Power quality enhancements became attainable when output voltage control methods were permitted. Verified by Ref. [34]. The authors of [35] investigate the application of asymmetrically switched Cascaded H-Bridge (CHB) multilevel inverters for photovoltaic systems. The study examines harmonic reduction methods for Total Harmonic Distortion (THD) mitigation and power quality improvements in solar powered systems while emphasizing lower part count and higher efficiency benefits.

The research investigates solar PV-fed PMBLDC motor control struggles caused by voltage changes and load variations that can be solved with Fractional-Order Proportional-Integral (FOPIλ) controllers. The use of Bat Algorithm (BA) and Grey Wolf Optimization (GWO) remains limited specifically for PV systems applications. The proposed study implements FOPIλ controller optimization through Whale Optimization Algorithm (WOA) which outperforms BA and GWO by minimizing time-domain parameters and convergence time and cost function along with successful PV power fluctuation and load disturbance management for renewable energy integrated motor control systems [36]. The researchers suggest implementing an MGA-based optimization of FOPID controllers for BLDC motor speed control under sensorless conditions. The MGA-FOPID controller defeats integer-order PID controllers at minimizing time-domain characteristics and performance indexes across different speed and load conditions as demonstrated through simulations and hardware experiments which leads to a reliable solution for BLDC motor control [37]. The study presents an Artificial Bee Colony (ABC)-optimized fractional-order PID (FOPID) controller for brushless DC (BLDC) motor control which targets settling time along with steady-state error stability problems. The ABC-tuned FOPID outperforms genetic algorithm-based controllers in time-domain characteristics and performance indices. Simulations have tested and experimentally confirmed how the Kalman Filter works as a speed estimator through Hall Effect sensor substitution [38]. The research proposes a Bat Algorithm (BA)-optimized Fractional-Order PID (FOPID) controller for sensorless BLDC motor speed control. The BA-tuned FOPID improves transient characteristics and minimizes steady-state error, outperforming ABC and MGA methods, offering a robust solution for enhanced motor performance [39].

This study builds upon previous research to develop a comprehensive understanding of MLIs with a minimal number of switches and reduced harmonic distortion. A novel configuration for a single-phase 49-level inverter is proposed and modeled, utilizing phase disposition level-shifted pulse width modulation (PDLSPWM)control technique. The proposed topology is designed to generate multiple output voltage levels with minimal THD. The control strategy is implemented to operate the switches in the proposed circuit effectively. The innovative feature of this design lies in its ability to achieve output voltage levels from 3 to 49 with a reduced number of switches, thereby enhancing the quality of the power circuit and significantly improving overall circuit efficiency.

3. Method

The suggested 49-level inverter circuit is illustrated in Fig. 1 and the direction of current of some different level is shown in Fig. 2,

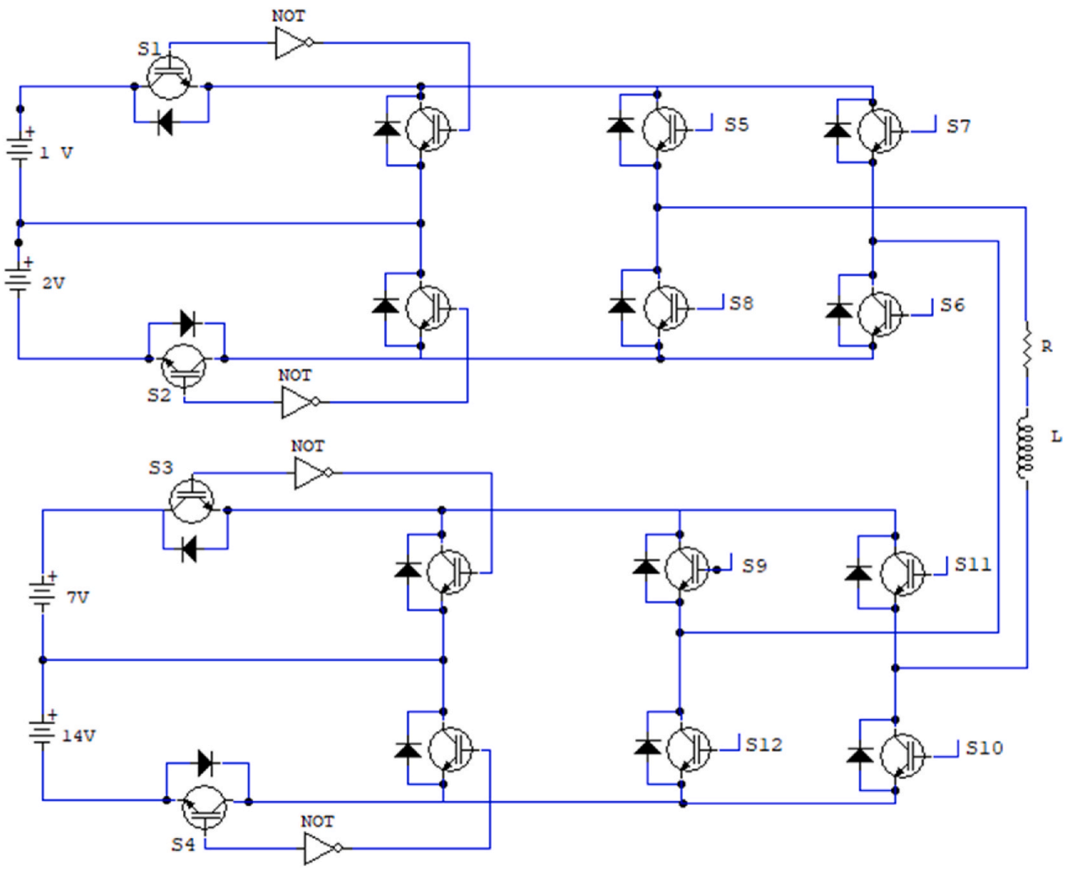

Fig. 1. Suggested 49-level inverter circuit.

Table 1
Switching patterns.

Output Level	S1	S2	S3	S4	S5	S6	S7	S8	S9	S10	S11	S12
0	0	0	0	0	1	0	1	0	1	0	1	0
1	1	0	0	0	1	1	0	0	1	0	1	0
2	0	1	0	0	1	1	0	0	1	0	1	0
3	1	1	0	0	1	1	0	0	1	0	1	0
4	1	1	1	0	0	0	1	1	1	1	0	0
5	0	1	1	0	0	0	1	1	1	1	0	0
6	1	0	1	0	0	0	1	1	1	1	0	0
7	0	0	1	0	1	0	1	0	1	1	0	0
8	1	0	1	0	1	1	0	0	1	1	0	0
9	0	1	1	0	1	1	0	0	1	1	0	0
10	1	1	1	0	1	1	0	0	1	1	0	0
11	1	1	0	1	0	0	1	1	1	1	0	0
12	0	1	0	1	0	0	1	1	1	1	0	0
13	1	0	0	1	0	0	1	1	1	1	0	0
14	0	0	0	1	1	0	1	0	1	1	0	0
15	1	0	0	1	1	1	0	0	1	1	0	0
16	0	1	0	1	1	1	0	0	1	1	0	0
17	1	1	0	1	1	1	0	0	1	1	0	0
18	1	1	1	1	0	0	1	1	1	1	0	0
19	0	1	1	1	0	0	1	1	1	1	0	0
20	1	0	1	1	0	0	1	1	1	1	0	0
21	0	0	1	1	1	0	1	0	1	1	0	0
22	1	0	1	1	1	1	0	0	1	1	0	0
23	0	1	1	1	1	1	0	0	1	1	0	0
24	1	1	1	1	1	1	0	0	1	1	0	0
−1	1	0	0	0	0	0	1	1	1	0	1	0
−2	0	1	0	0	0	0	1	1	1	0	1	0
−3	1	1	0	0	0	0	1	1	1	0	1	0
−4	1	1	1	0	1	1	0	0	0	0	1	1
−5	0	1	1	0	1	1	0	0	0	0	1	1
−6	1	0	1	0	1	1	0	0	0	0	1	1
−7	0	0	1	0	1	0	1	0	0	0	1	1
−8	1	0	1	0	0	0	1	1	0	0	1	1
−9	0	1	1	0	0	0	1	1	0	0	1	1
−10	1	1	1	0	0	0	1	1	0	0	1	1
−11	1	1	0	1	1	1	0	0	0	0	1	1
−12	0	1	0	1	1	1	0	0	0	0	1	1
−13	1	0	0	1	1	1	0	0	0	0	1	1
−14	0	0	0	1	1	0	1	0	0	0	1	1
−15	1	0	0	1	0	0	1	1	0	0	1	1
−16	0	1	0	1	0	0	1	1	0	0	1	1
−17	1	1	0	1	0	0	1	1	0	0	1	1
−18	1	1	1	1	1	1	0	0	0	0	1	1
−19	0	1	1	1	1	1	0	0	0	0	1	1
−20	1	0	1	1	1	1	0	0	0	0	1	1
−21	0	0	1	1	1	0	1	0	0	0	1	1
−22	1	0	1	1	0	0	1	1	0	0	1	1
−23	0	1	1	1	0	0	1	1	0	0	1	1
−24	1	1	1	1	0	0	1	1	0	0	1	1

the references for the mathematical data and equations have been appropriately provided immediately before each equation to ensure proper attribution and clarity. The power circuit is designed that the values of DC sources are unequal with different arrangement ratio and less switches (SWs), the highest SW and DC sources to acquire N-level output voltages for traditional multilevel inverter are calculated as [40]:

$$\text{No. of SW} = 2(\text{N} - 1) \tag{1}$$

$$\text{No. of DC source} = (\text{N} - 1)\ /2 \tag{2}$$

So, to have 49 output voltage level, the circuit needs 96 SW and 24 DC sources. While for the suggested multilevel inverter, number of SWs and DC sources to get 49-level output voltage are calculated as:

$$\text{No. of SW} = (\text{N} - 1)\ /\ 4 \tag{3}$$

$$\text{No. of DC source} = (\text{N} - 9)\ /\ 10 \tag{4}$$

According to equations (3) and (4), number of required SW is 12 and number of DC sources is 4 and its switching states (S1 to S12) with their 49 output levels is explained in Table 1.

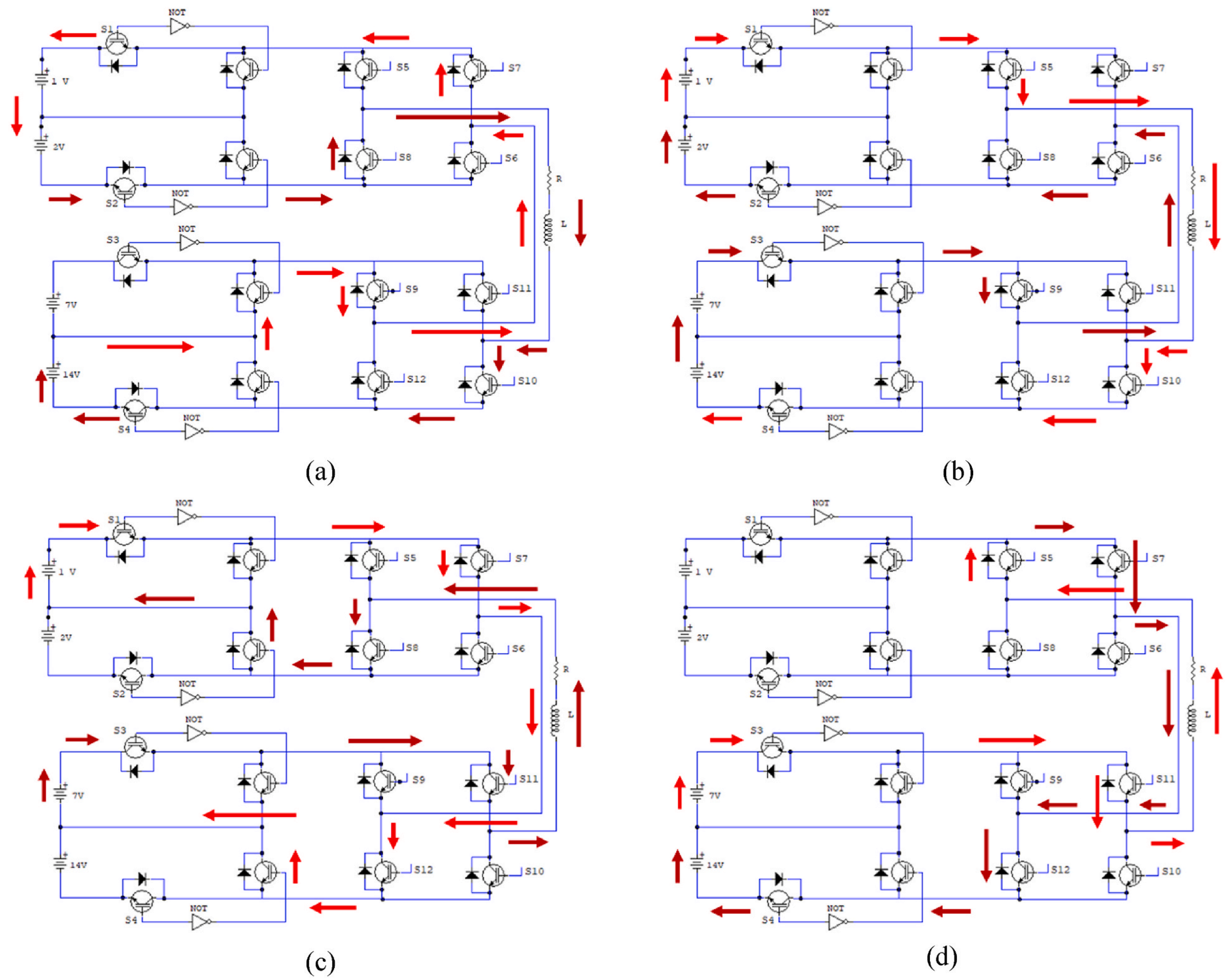

Fig. 2. Current path of 49-level output voltage inverter to produce (a) 11-level (b) 24-level (c) -8-level, and (d) −24-level.

the suggested power circuit is designed to generate multiple output voltages by switching switches ON and OFF simultaneously. Voltage sources (1, 2, 7, and 14) Vdc are summed or subtracted by switches at different combinations. The PDLSPWM (Phase-Disposed Level-Shifted Pulse Width Modulation) control technique is a modulation method used in multilevel inverters to generate the appropriate switching signals for the inverter's power devices. This technique divides the total number of voltage levels into phases and then shifts each phase to produce the desired waveform. In comparison to other modulation techniques, such as Sinusoidal PWM (SPWM) and Space Vector PWM (SVPWM), PDLSPWM offers several advantages. First of all; **Improved Harmonic Performance**: PDLSPWM helps reduce Total Harmonic Distortion (THD) in both the output voltage and current by optimizing the switching sequence and phase displacement. This leads to higher-quality power with less harmonic content. Furthermore; **Reduced Switching Losses**: the technique minimizes the number of switching events by using level-shifted signals, which helps reduce switching losses in power devices, particularly in high-voltage applications. In addition to what mentioned, **Better Voltage Balancing is another advantage**: It ensures better voltage balancing in multilevel inverters, which is crucial for maintaining the performance and efficiency of the system. Finally; **Increased Efficiency**: By improving the voltage waveform quality and reducing the number of switches, PDLSPWM enhances the overall efficiency of the system, making it suitable for both medium- and high-voltage applications.

In summary, PDLSPWM stands out due to its ability to provide high-quality output with reduced harmonic distortion and lower switching losses, making it an ideal choice for multilevel inverters compared to other conventional modulation techniques. It is very highly efficient in generating multiple voltage levels that makes it a good design for applications as motor drives, renewable energy systems, and power conditioning due to its asymmetrical cascaded inverter design. In addition to improving output waveform quality, the retained control over the state of the switch minimizes THD increasing overall system performance.

4. Results and discussion

To certify the importance of the projected MLI circuit capabilities, simulation results by MATLAB program are discussed with input

DC voltage sources of three cases:

- case 1; Working with per unit system (1:2:7:14) volt and power factor (PF)of 0.62.
- Case 2: Working with actual voltages, (40:80:280:560) volt and PF of 0.94.
- Case 3: Replacing batteries with PVs and the output of the PV-boost circuits equal to (40:80:280:560) volt with PF of 0.62.

4.1. Case 1

Working with per unit system (1:2:7:14) volt and PF of 0.62. The MATLAB circuit model of the proposed 49-level inverter system is illustrating in Fig. 3. The table below demonstrates the impact of increasing voltage levels on the harmonic distortion and power quality of the suggested asymmetrical 49-level inverter circuit. By using voltage ratios of 1:2:7:14, the inverter achieves a wide range of output levels with improved waveform quality at higher levels. The highlighted levels in Table 2 are selected to illustrated the output

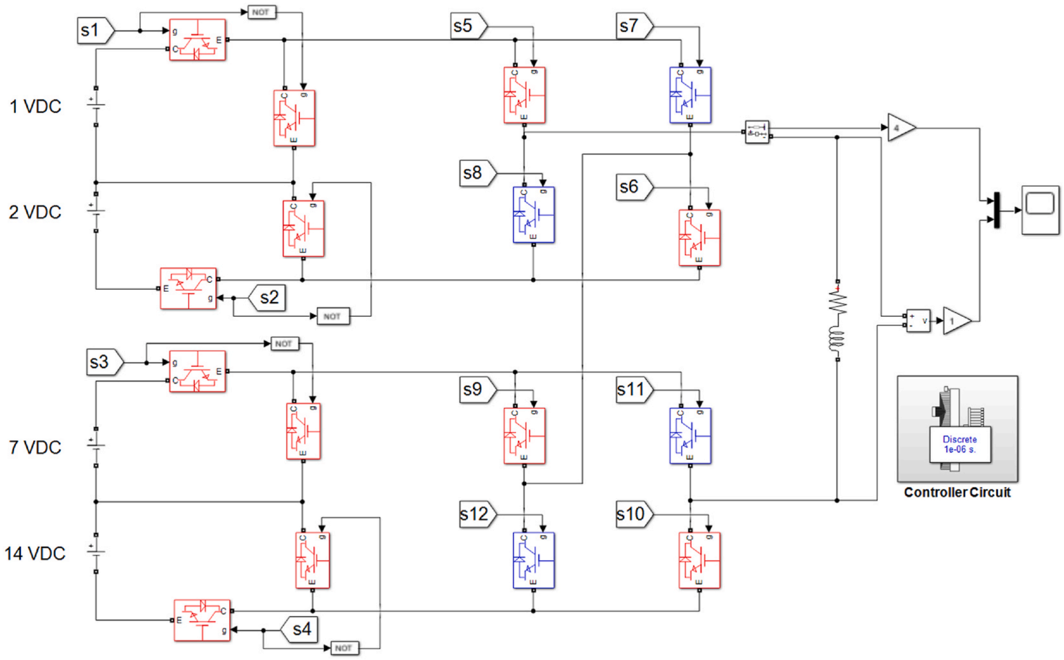

Fig. 3. Modeling of proposed 49-level inverter system fed by battery DC sources.

Table 2
Result of THDvo THDio and powers in range 11–49 levels.

Level	THDvo	THDio	S P Q D
11	1.4771	0.5496	2.3337 1.4556 1.8238 0.0323
13	1.683	0.22947	3.3595 2.0964 2.6246 0.0542
15	1.345	0.094932	4.5750 2.8537 3.5753 0.0585
17	1.4325	0.16846	5.9733 3.7236 4.6699 0.0801
19	1.3189	0.33548	7.5627 4.7142 5.9129 0.0879
21	1.3517	1.1853	9.3365 5.8284 7.2932 0.0993
23	1.1431	0.55705	11.2973 7.0478 8.8286 0.1086
25	1.1493	0.67153	13.4448 8.3829 10.5105 0.1359
27	0.96522	0.44361	15.7781 9.8422 12.3312 0.1398
29	0.90939	0.10788	18.3026 11.4120 14.3083 0.1548
31	0.92435	0.45305	21.0048 13.1025 16.4163 0.1796
33	0.87329	0.28978	23.8957 14.9069 18.6749 0.1969
35	0.80437	0.13902	26.9712 16.8243 21.0796 0.2017
37	0.93269	0.21304	30.2345 18.8569 23.6322 0.2565
39	0.92925	0.25061	33.6531 21.0002 26.2953 0.2791
41	0.87209	0.20382	37.4035 23.3444 29.2229 0.2868
43	0.61887	0.30332	41.2108 25.7024 32.2128 0.2316
45	0.82137	0.22038	45.0739 28.1258 35.2205 0.3265
47	0.5978	0.21859	49.4309 30.8288 38.6383 0.2719
49	0.71216	0.093319	53.8115 33.5819 42.0452 0.3589

voltage and current with their spectrum analysis. This table explains the THD_{Vo}, THD_{Io}, apparent power (S), real power (P), reactive power (Q), and distortion power (D). The analysis confirms the suitability of this design for applications requiring high power quality, such as motor drives and renewable energy systems.

The output voltage and current with its FFT spectrum of the recommended 11, 21, 31, 41 and 49-level inverter using PDLSPWM technique are shown in Figs. 4–8, respectively. The THD values of the output voltage and current for these levels are (1.4771 %, 0.5496 %), (1.5317 %, 1.1853 %), (0.92435 %, 0.45305 %), (0.87209 %, 0.20382 %) and (0.71216 %, 0.093319 %), respectively. The performance analysis reveals that the 49-level asymmetrical inverter achieves significant improvements in harmonic distortion, power delivery, and waveform quality as the number of levels increases. Fig. 9 shows the THD of the output voltage and current at different voltage levels. These results are confirmed by the distortion power demonstrated in Figure (10d). The S, P, and Q waveforms explained

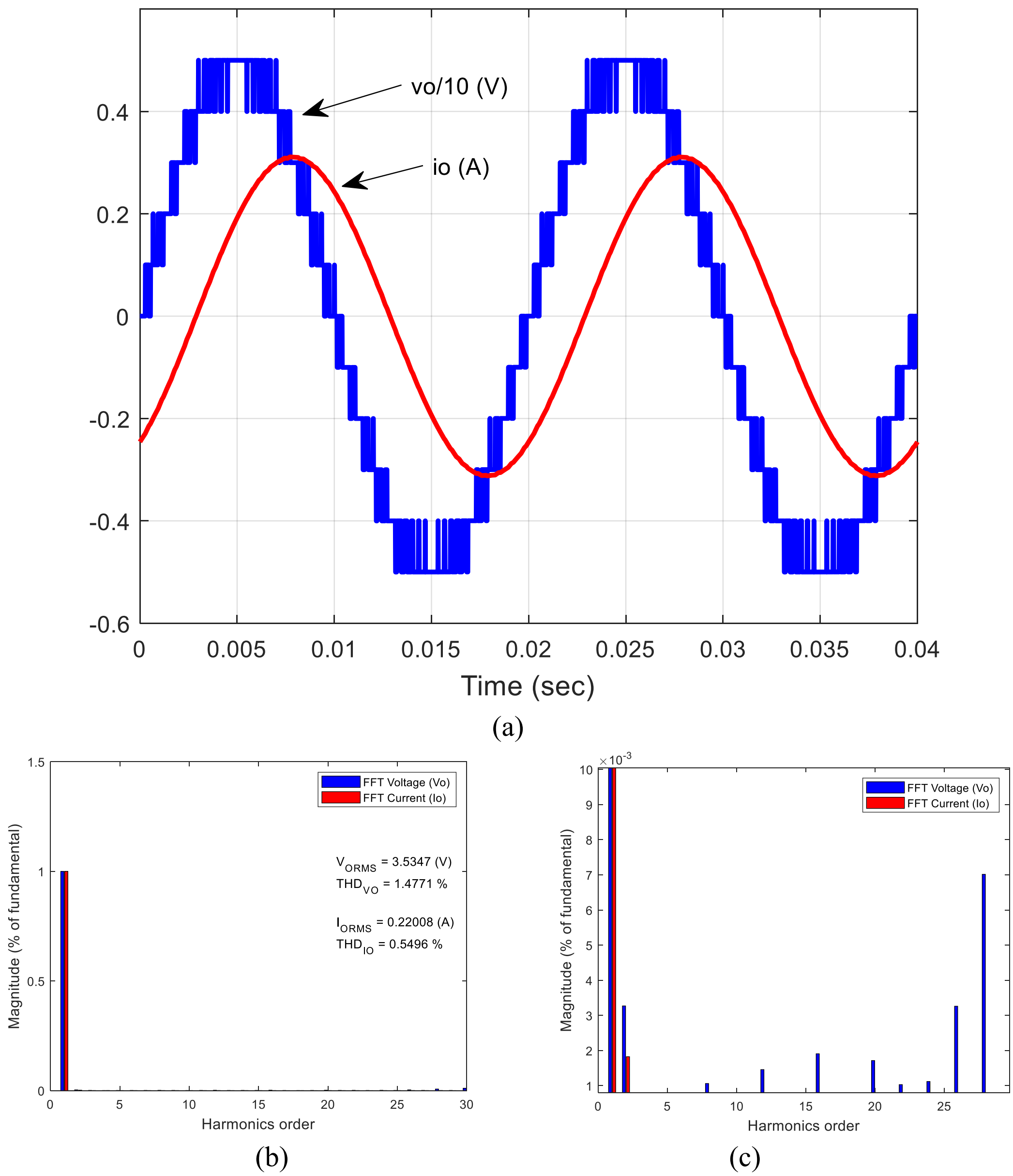

Fig. 4. Simulation results of the 11-level (a) output phase voltage and current with its (b) spectrum analyzer and (c) zoom section for the low harmonics order.

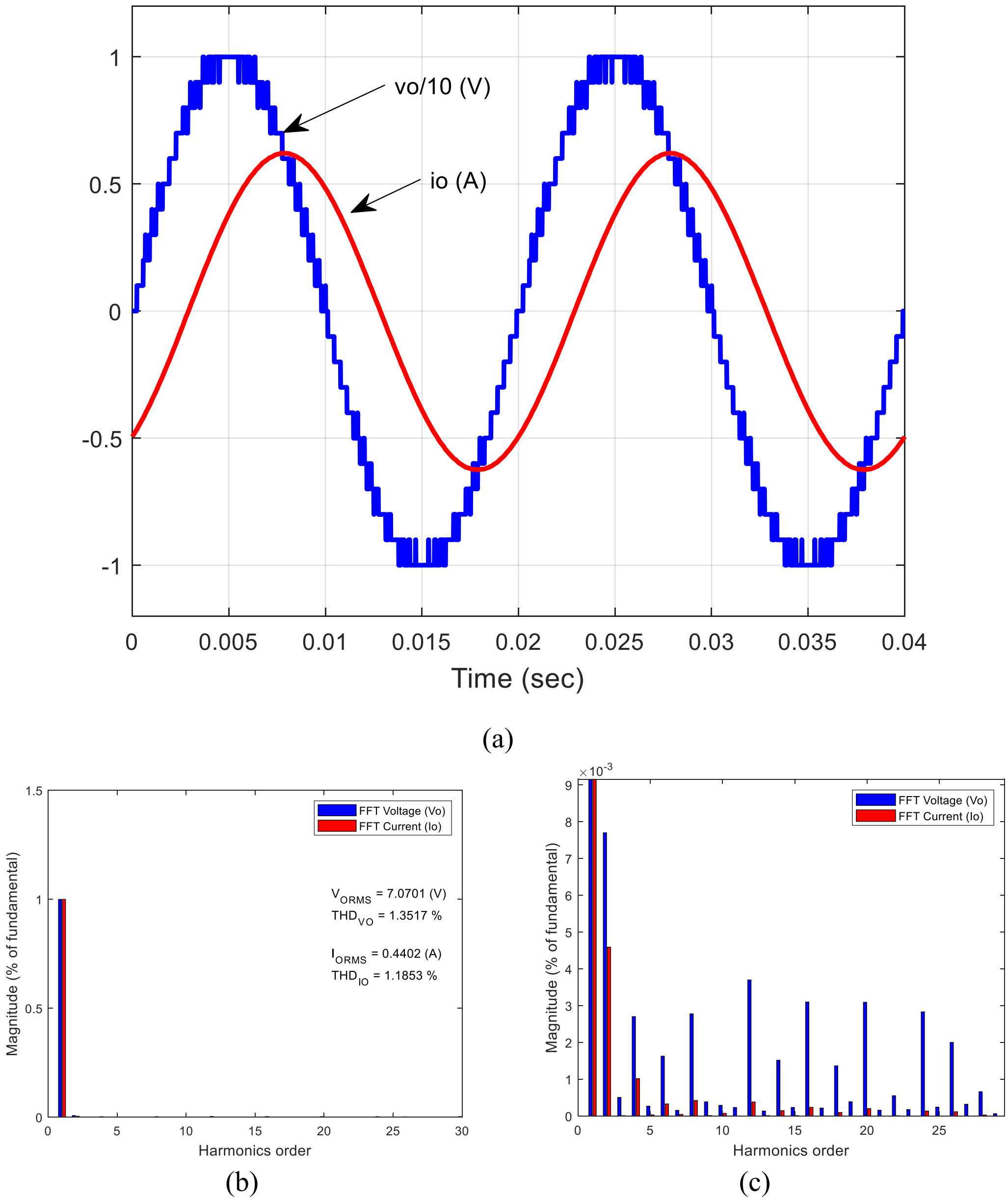

Fig. 5. Simulation results of the 21-level (a) output phase voltage and current with its (b) spectrum analyzer and (c) zoom section for the low harmonics order.

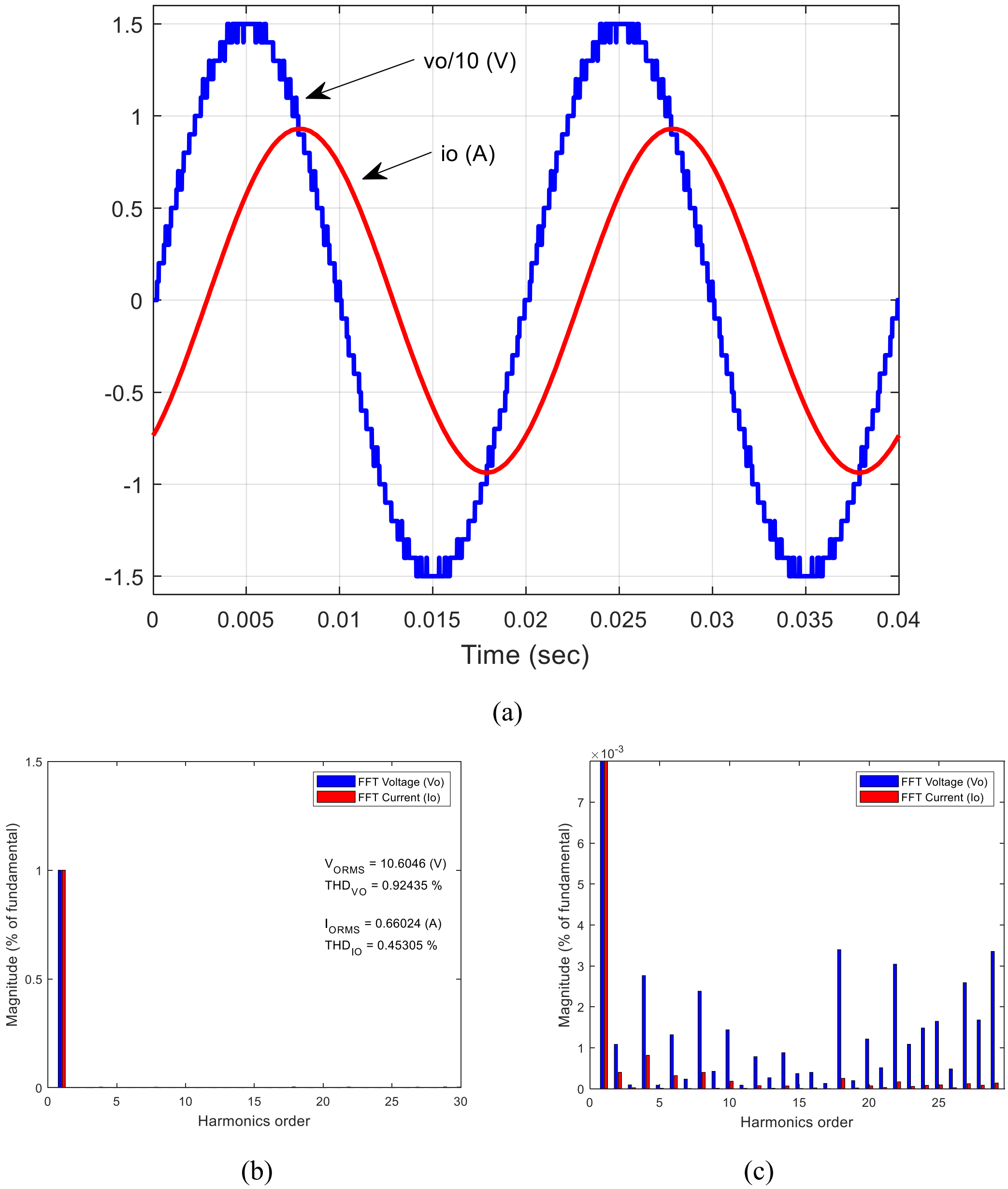

Fig. 6. Simulation results of the 31-level (a) output phase voltage and current with its (b) spectrum analyzer and (c) zoom section for the low harmonics order.

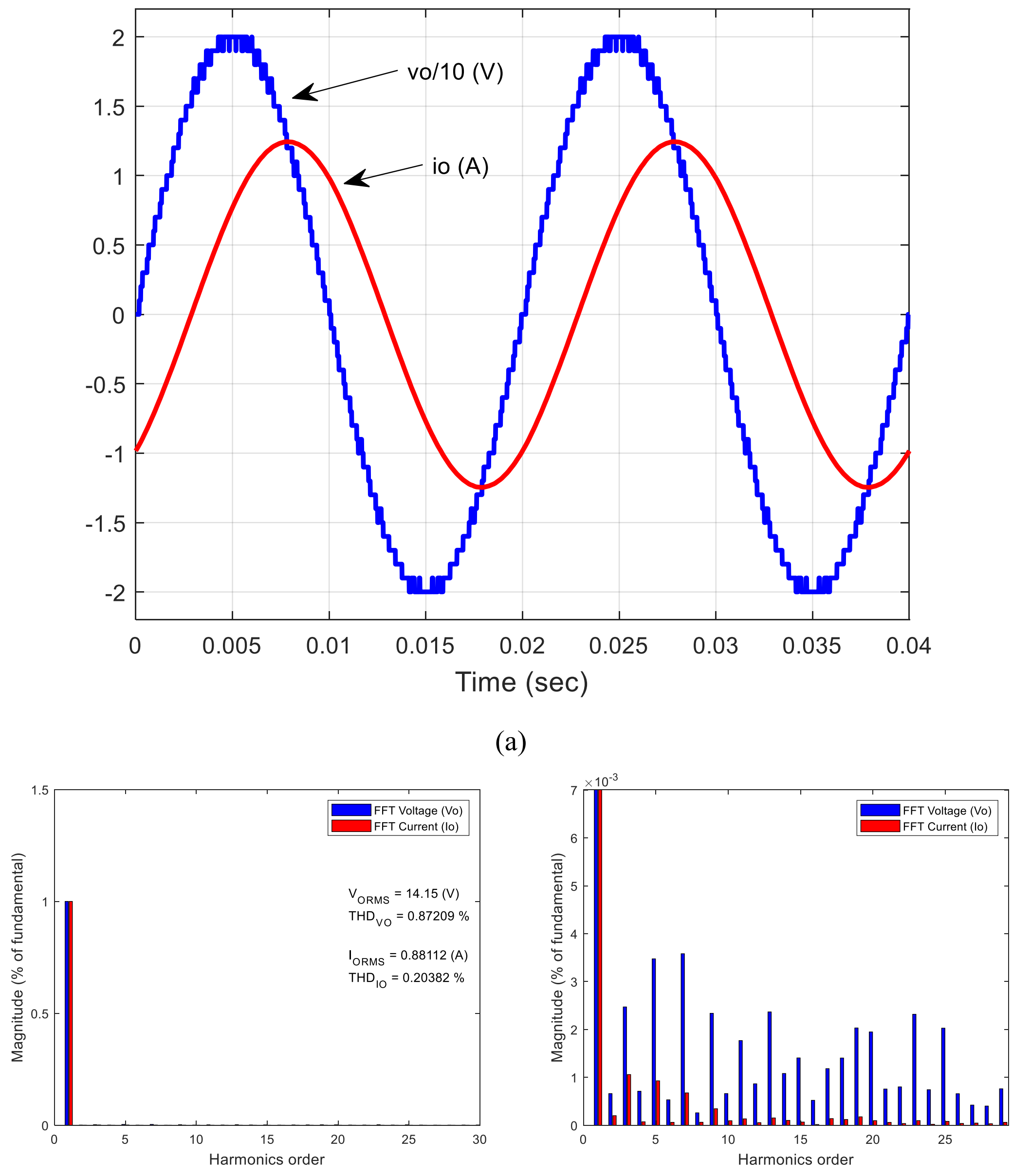

Fig. 7. Simulation results of the 41-level (a) output phase voltage and current with its (b) spectrum analyzer and (c) zoom section for the low harmonics order.

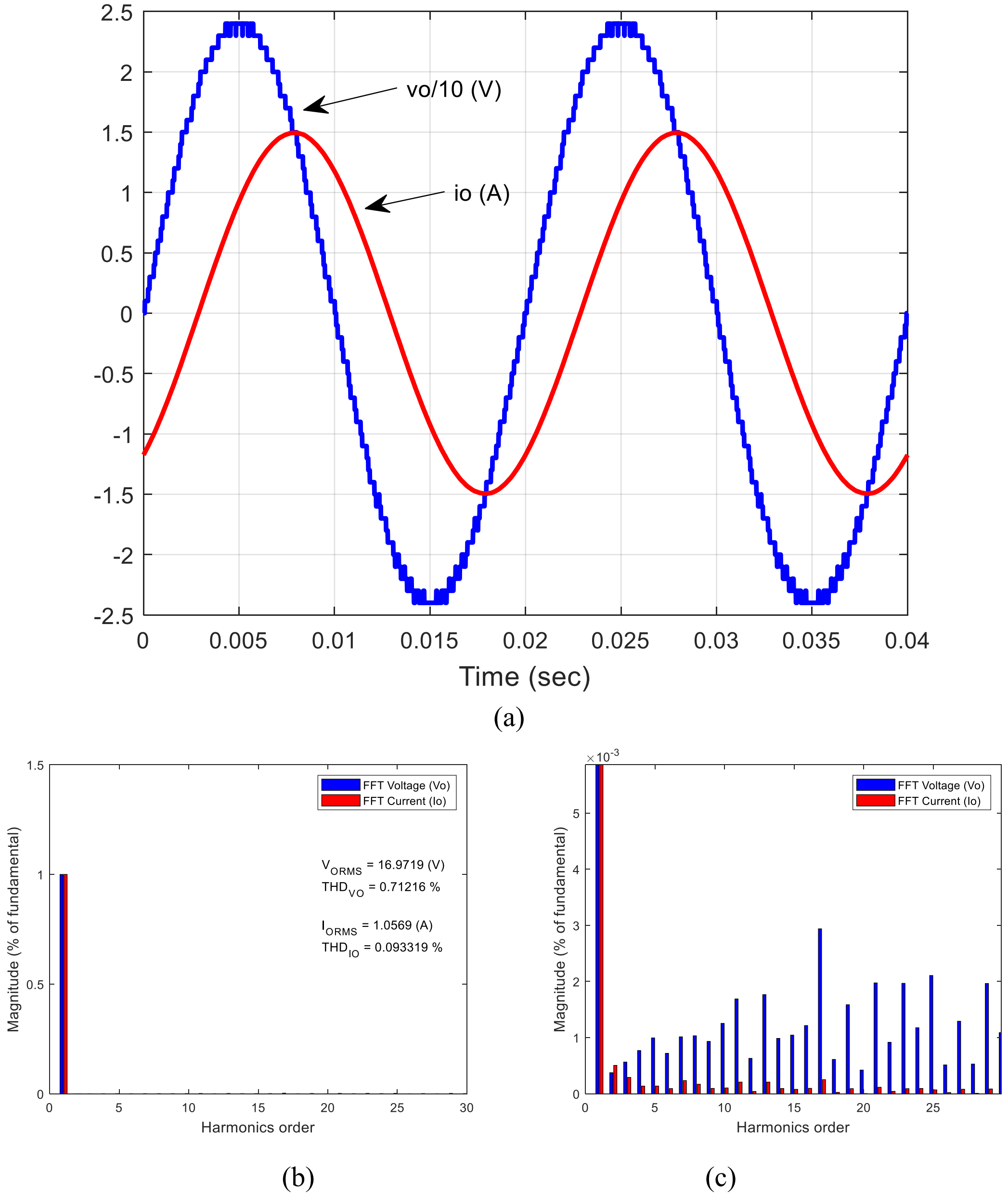

Fig. 8. Simulation results of the 49-level (a) output phase voltage and current with its (b) spectrum analyzer and (c) zoom section for the low harmonics order.

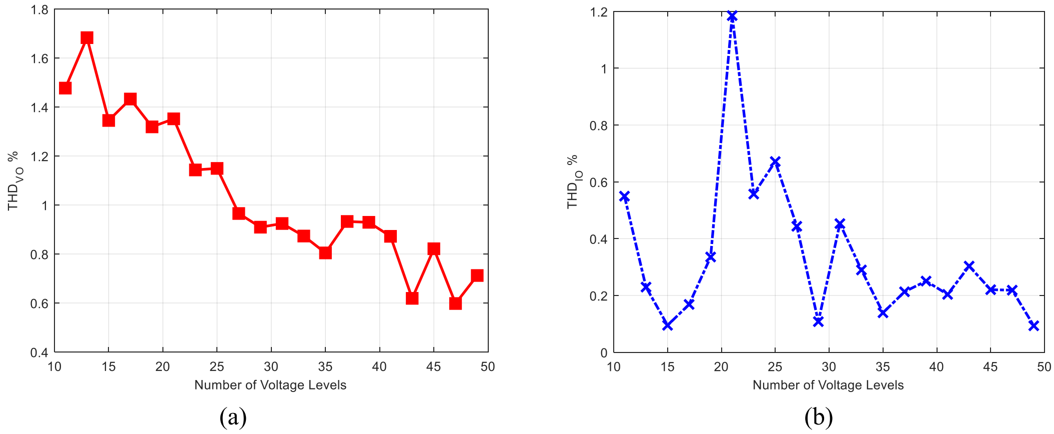

Fig. 9. THD of the output (a) voltage and (b) current of the multilevel.

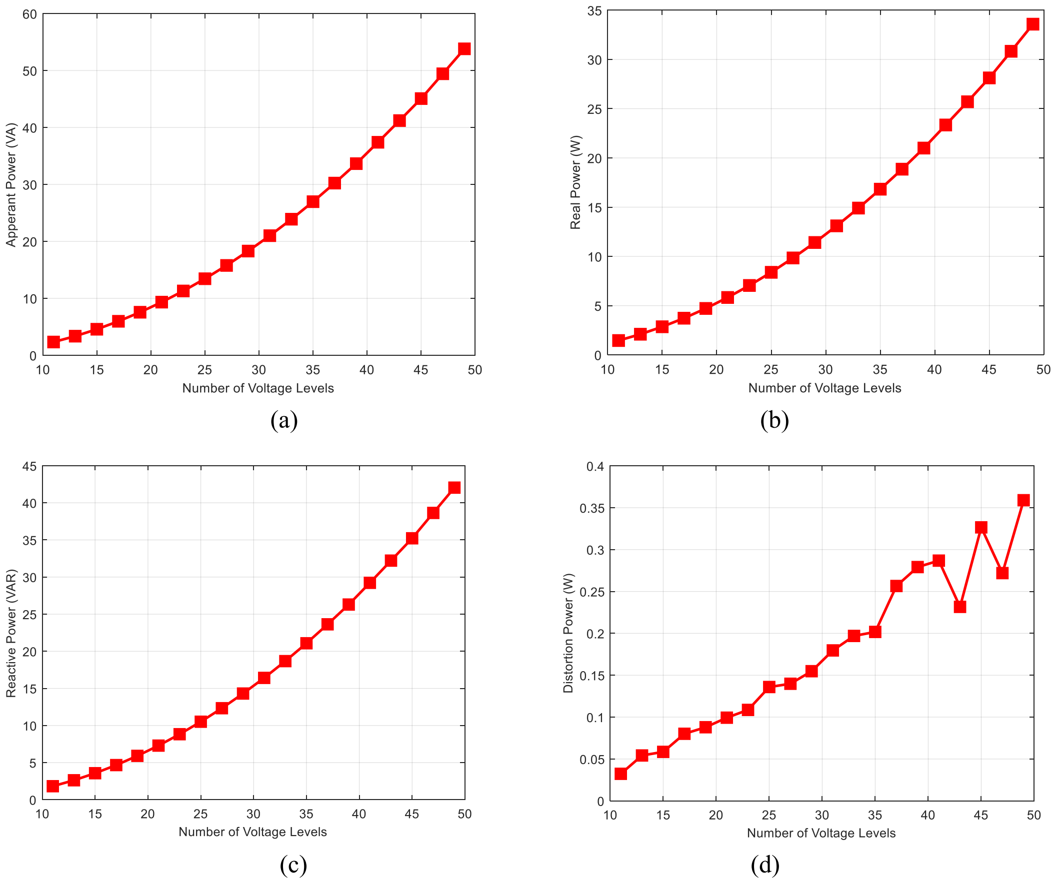

Fig. 10. (a) Apparent power, (b) real power, (c) reactive power and (d) distortion power.

in Fig. 10 show the that these powers increased by increasing voltage levels. The overall results prove the effectiveness of the designed

Table 3
Result of THD_{Vo}, THD_{Io}, and powers.

Level	THDvo	THDio	S P Q D
11	1.4766	0.45555	376.7927 355.1100 125.8716 5.0973
13	1.6827	0.2861	542.4374 511.2738 181.0022 8.6970
15	1.3447	0.21384	738.6406 696.1473 246.7380 9.4417
17	1.4324	0.30123	964.4265 908.7828 322.5958 12.8195
19	1.3185	0.53715	1221.1 1150.6408.5 13.8
21	1.3513	1.0172	1507.5 1421.1502.8 12.6
23	1.1429	0.59674	1824.1 1719.3609.2 15.5
25	1.1489	0.58062	2170.8 2045.8725.9 19.7
27	0.96482	0.38449	2547.6 2401.1851 21.3
29	0.9089	0.20905	2955.1 2784.9988.1 24.5
31	0.92393	0.37004	3391.4 3196.4 1132.9 27.2
33	0.8731	0.26052	3858.2 3636.5 1288.6 31
35	0.80387	0.20355	4354.8 4104.5 1454.8 32.2
37	0.9318	0.29779	4881.7 4600.9 1631.4 40.7
39	0.92674	0.38639	5433.7 5121.9 1813.7 44.7
41	0.87057	0.33944	6039.3 5693.1 2015 43.6
43	0.61766	0.26991	6653.8 6271.1 2223.7 34.9
45	0.8221	0.3189	7277.6 6860 2429.4 50.4
47	0.59736	0.21145	7981.1 7522.1 2667.3 41.9
49	0.71227	0.16719	8688.5 8190.2 2899.7 56.8

power circuit and controller.

4.2. Case2

Working with actual voltages (40:80:280:560) volt and PF of 0.94.

The highlighted voltage levels explained in Table 3 are selected and plotted with their spectrum analysis. The analysis confirms the suitability of this design circuit.

The output voltage and current waveforms with their FFT analysis at different selected levels are explained in Figs. 11–15, respectively. The THD values of the output voltage and current for these levels are (1.4766 %, 0.45555 %), (1.3515 %, 1.0172 %), (0.92393 %, 0.37004 %), (0.87057 %, 0.33944 %) and (0.71227 %, 0.16719 %), respectively. Fig. 16 shows the THD waveforms of the output voltage and current at different voltage levels. These results are proved by the distortion power shown in Figure (17d). The S, P, and Q waveforms in Fig. 17 illustrate that these powers rise with rising the voltage levels. These results also prove the effectiveness of the designed power circuit and controller during this case.

To check the strength point of the designed power circuit and controller, the system tests the dynamic behavior of the output voltage and current over a time interval ranging. The inverter operates progressively across varying voltage levels, starting from 13 levels and incrementing by 4 levels at 0.2-s intervals, ultimately reaching 49 levels. Fig. 18 proves that it works properly in various level and different times continuously.

4.3. Case 3

In this case all batteries are replaced by PVs with outputs equal to (40:80:280:560) volt and PF of 0.62. The MLI is adapted and compatible to work with PVs as inputs as explained in Fig. 19. The results validate the inverter's ability to deliver high quality power with negligible harmonic distortion in the face of varying input conditions (irradiance), which make it a natural fit for modern energy applications, including smart grids, off grid systems, and renewable energy integration.

Fig. 20 illustrates the performance and characteristics (V-I and P-V) of a PV module that utilized as the input power source instead of conventional DC sources. The output voltage and current waveforms with the FFT spectrums of the recommended 49-level inverter using PDLSPWM technique and PF of 0.62 are shown in Fig. 21. The THD values of the output voltage and current are 1.2926 % and 0.33963 %.

Table 4 shows the three cases differ strongly in their voltage levels and power factor measurements and THD performance outcomes. The per-unit system in Case 1 (1:2:7:14) produces a minimum THD yet operates with a power factor at 0.62 while the THD values in case 3 are maximum, this discrepancy arises due to the error margin in the output voltage values from the PV boost circuit. The expected voltage levels are (40, 80, 280, and 560) V; however, the measured values were (37, 85, 298, and 580) V. consequently, this deviation led to an increase in the THD values compared to the cases utilizing batteries (case 1 and case 2). The examination only used a PV unit at 25 °C ambient temperature under 1000 W/m^2 radiation conditions but ignored the effects of changing temperatures and radiation levels. The future analysis will thoroughly evaluate this system's performance regarding these changing conditions.

Table 5 shows a comparison table between the proposed and suggested power circuit and controller with other references. The comparisons are done based on levels, no. of switches, no. of diodes, input source type, and THD of the output voltage and current. The proposed circuit is particularly suitable for the new and renewable energy systems and industrial applications where accuracy of performance and power quality have paramount importance such as large-scale renewable energy integration and smart grid systems.

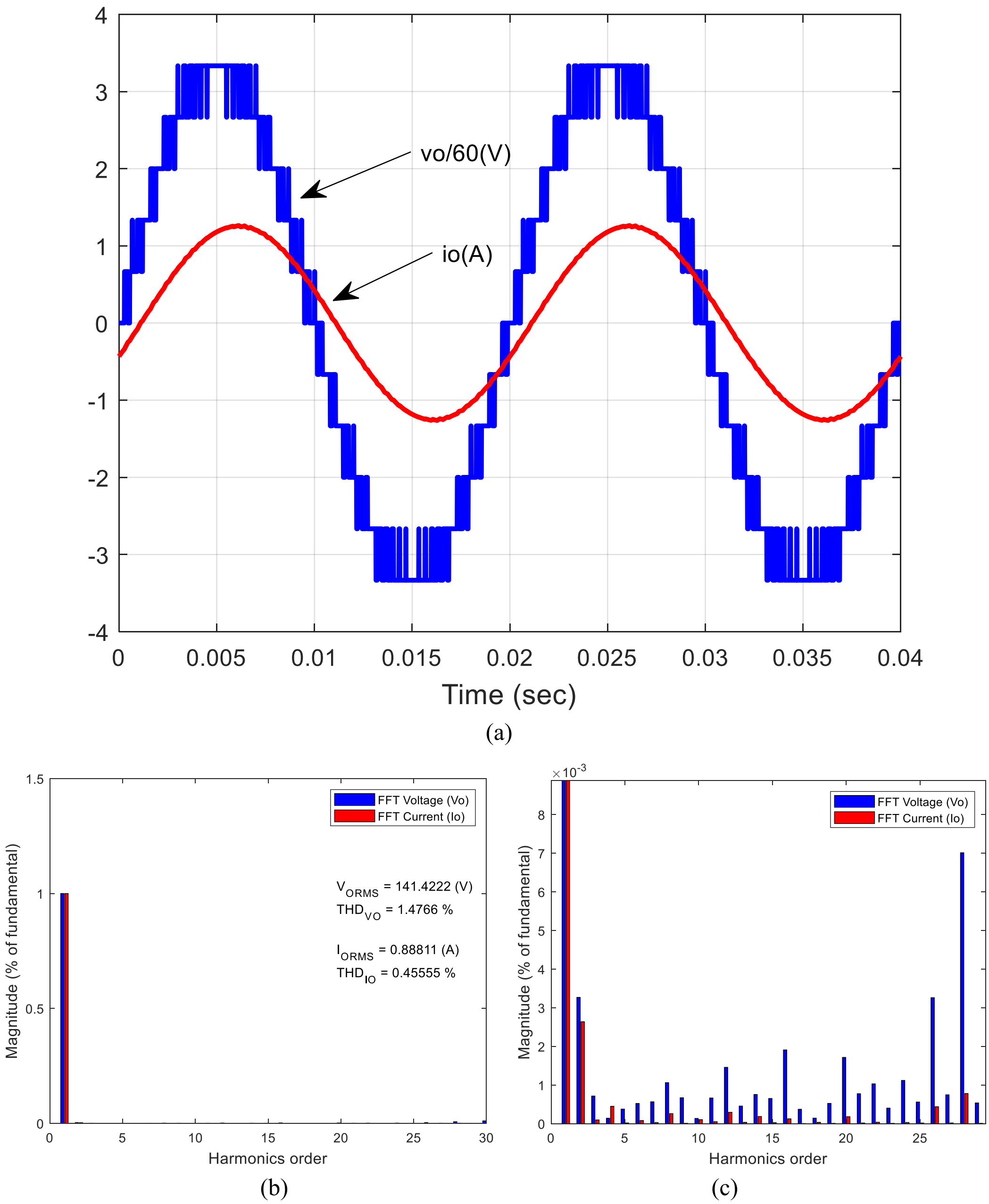

Fig. 11. Simulation results of the 11-level (a) output phase voltage and current with its (b) spectrum analyzer and (c) zoom section for the low harmonics order.

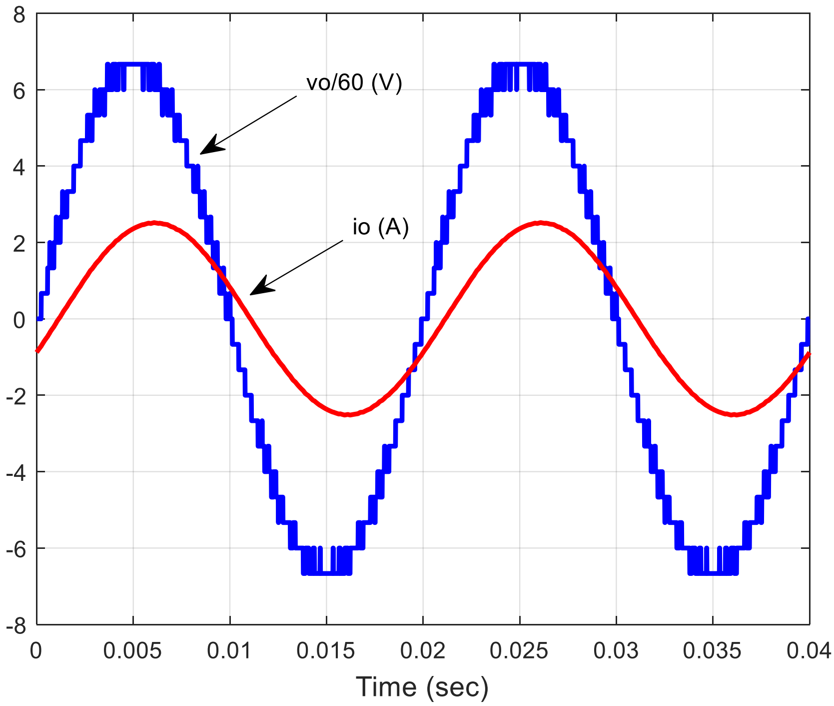

(a)

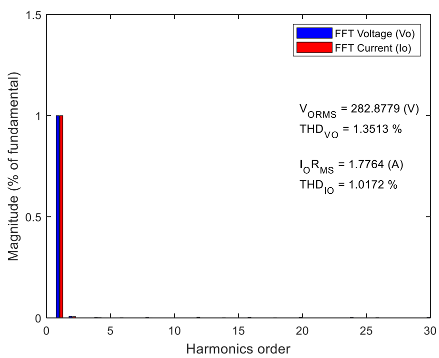

(b)

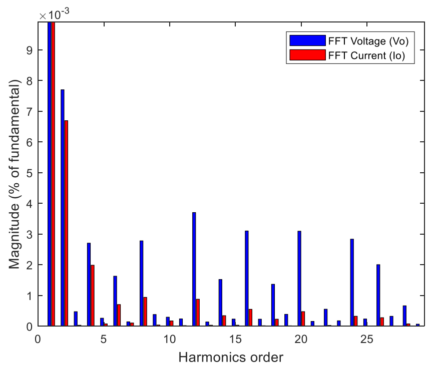

(c)

Fig. 12. Simulation results of the 21-level (a) output phase voltage and current with its (b) spectrum analyzer and (c) zoom section for the low harmonics order.

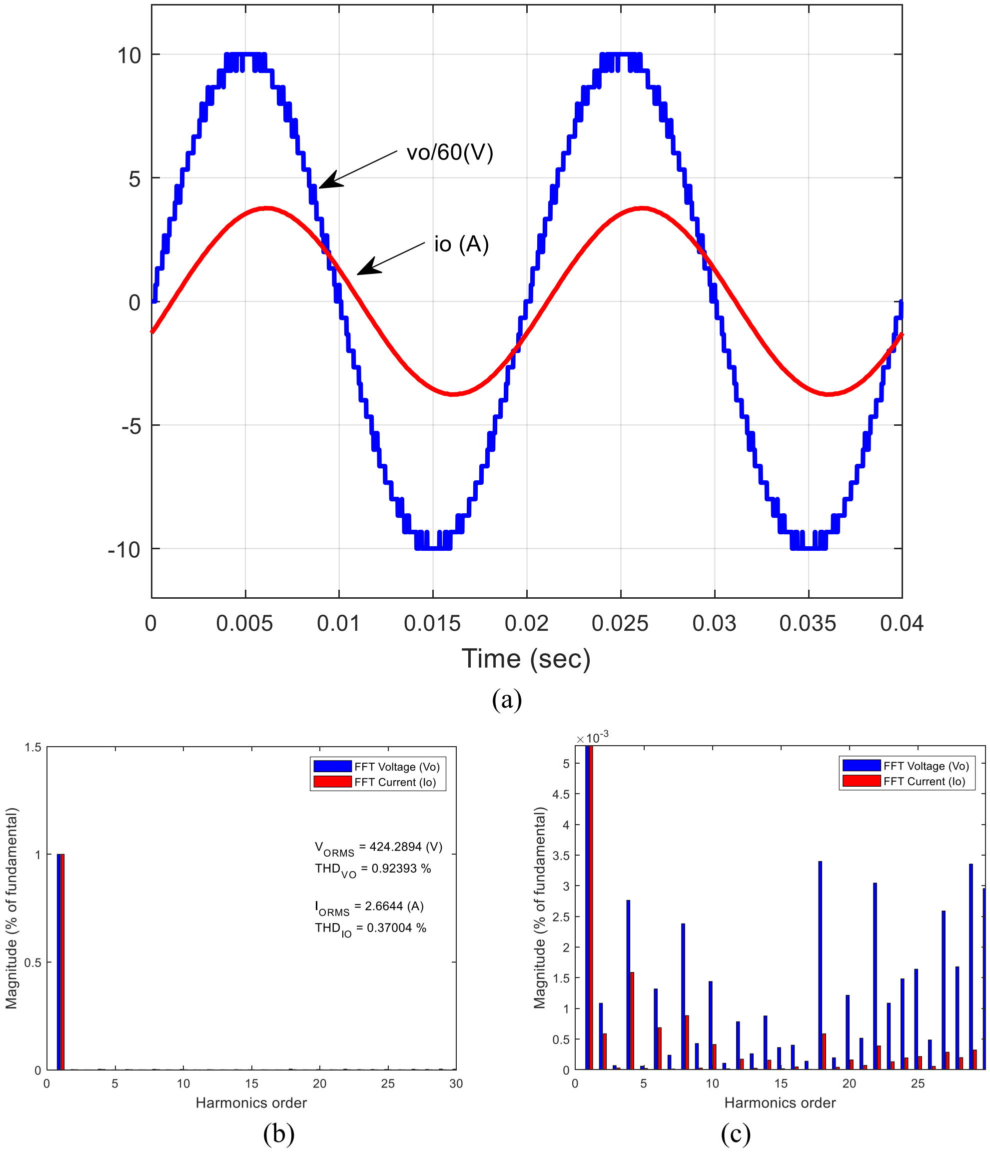

Fig. 13. Simulation results of the 31-level (a) output phase voltage and current with its (b) spectrum analyzer and (c) zoom section for the low harmonics order.

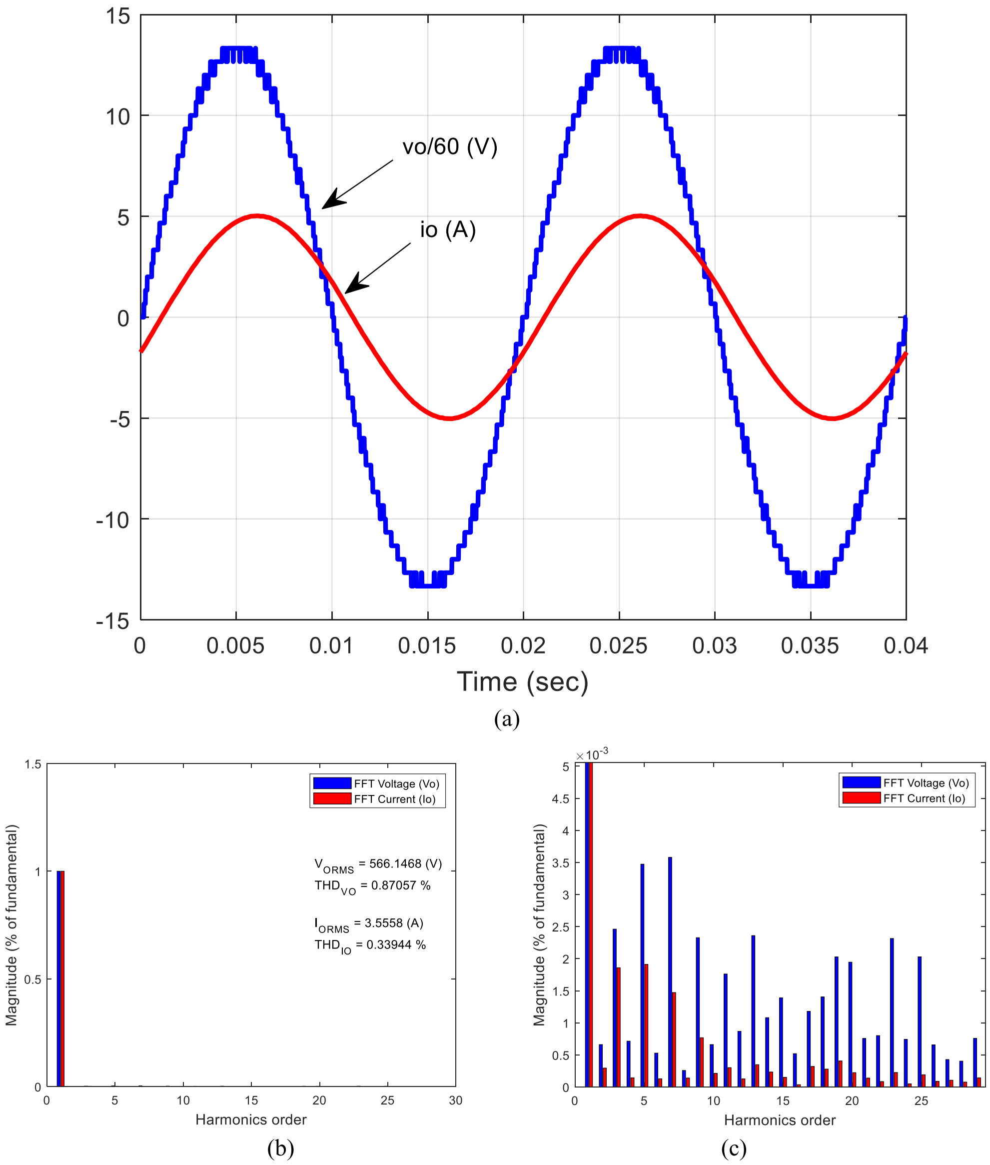

Fig. 14. Simulation results of the 41-level (a) output phase voltage and current with its (b) spectrum analyzer and (c) zoom section for the low harmonics order.

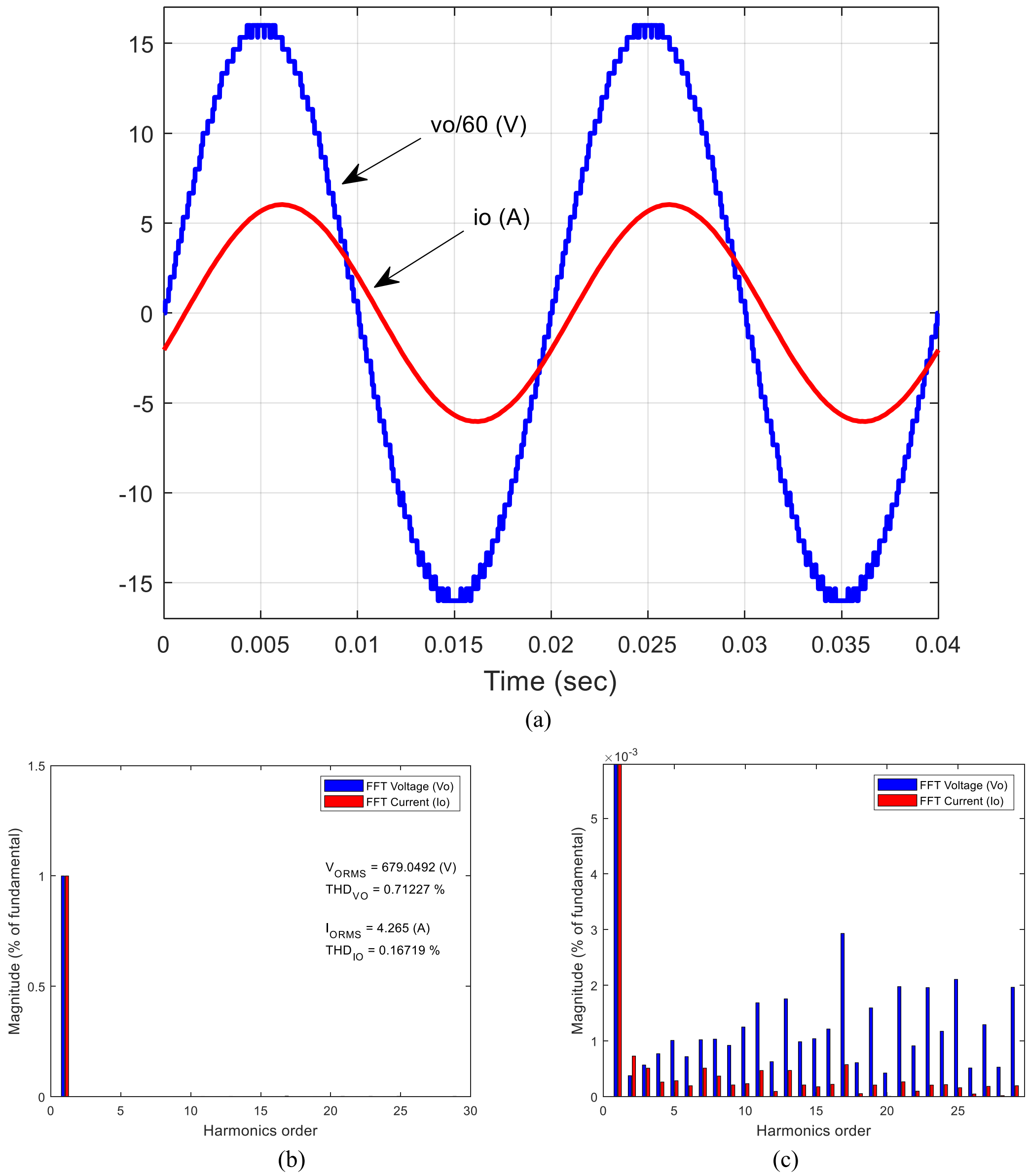

Fig. 15. Simulation results of the 49-level (a) output phase voltage and current with its (b) spectrum analyzer and (c) zoom section for the low harmonics order.

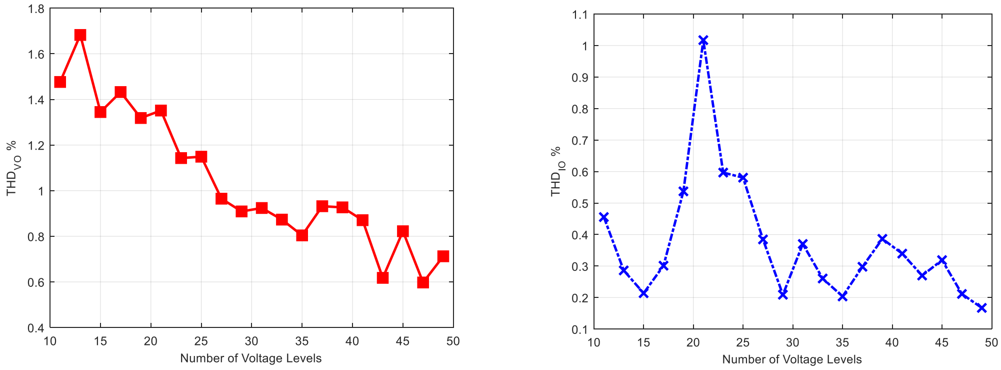

(a) (b)

Fig. 16. THD of the output (a) voltage and (b) current of the multilevel.

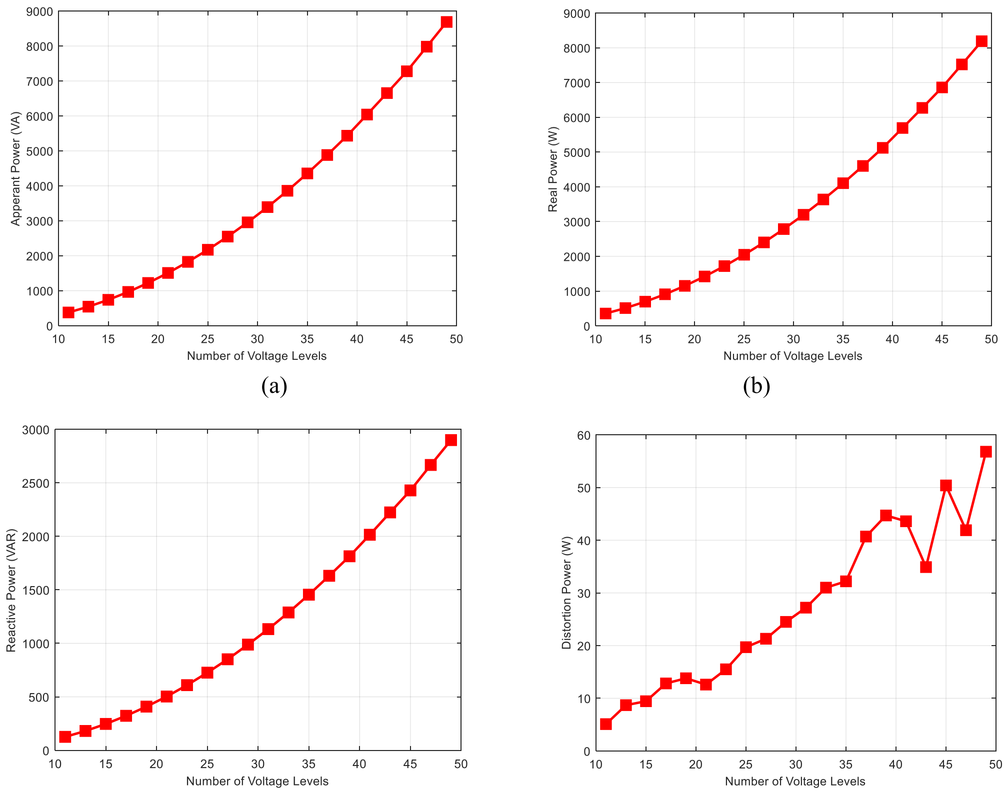

(c) (d)

Fig. 17. (a) Apparent power, (b) real power, (c) reactive power and (d) distortion power.

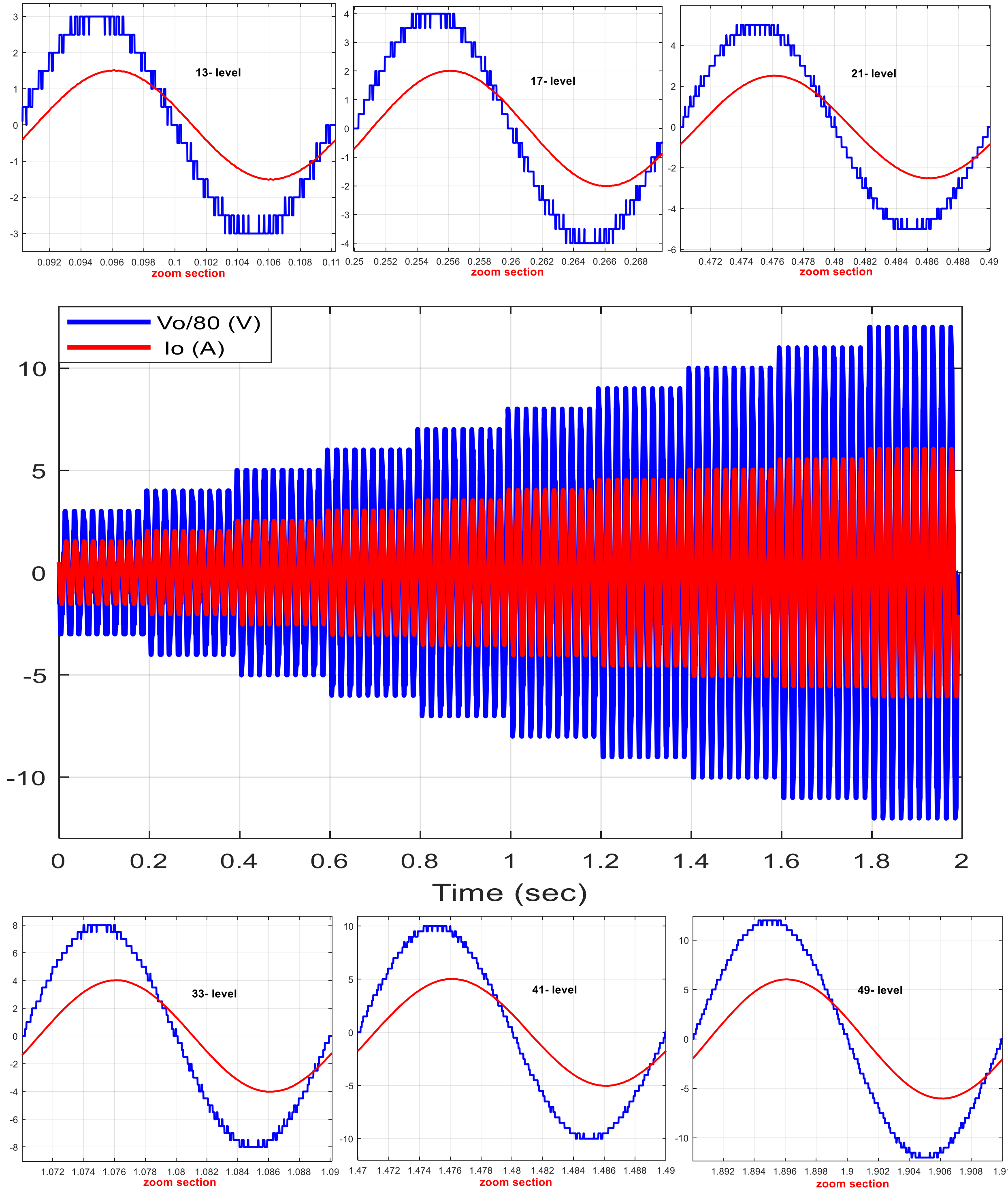

Fig. 18. Different output voltage and current of the proposed MLI.

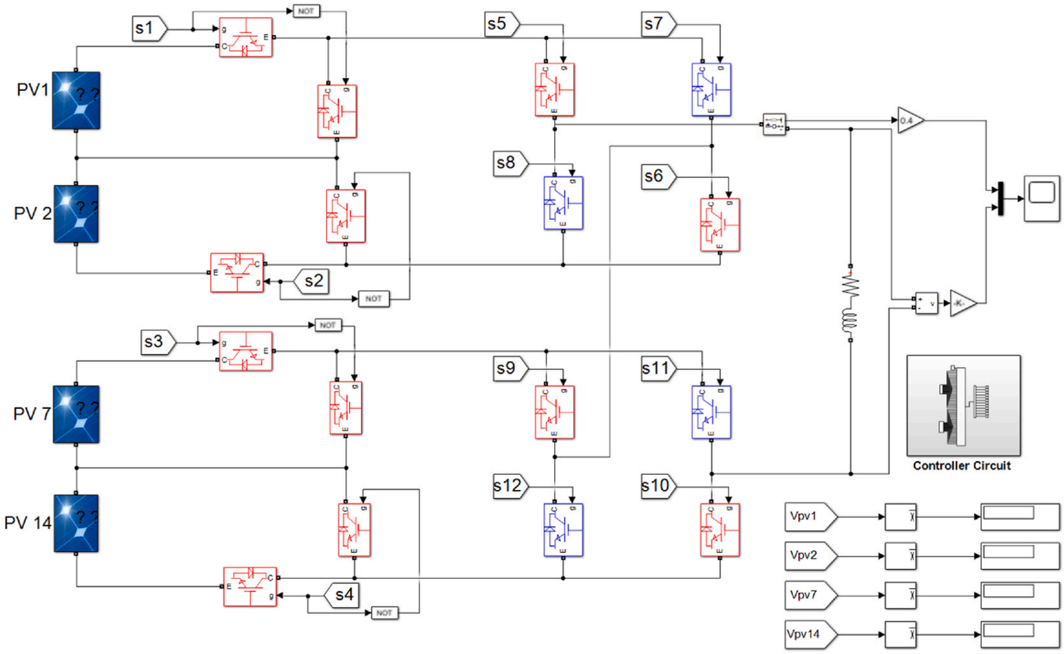

Fig. 19. Modeling of proposed 49-level inverter system fed by PV sources.

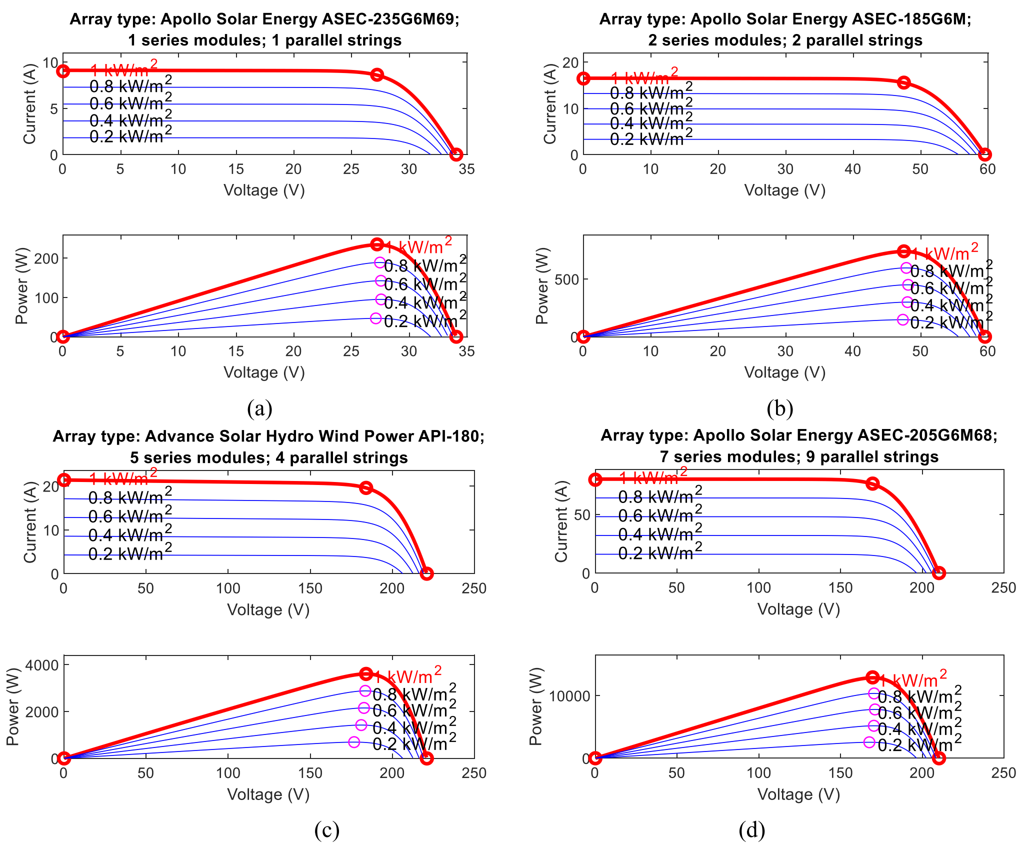

Fig. 20. The V-I and P-V characteristics of the solar panels (a) PV source 40V, (b) PV source 80V, (c) PV source 280V and (d) PV source 560V.

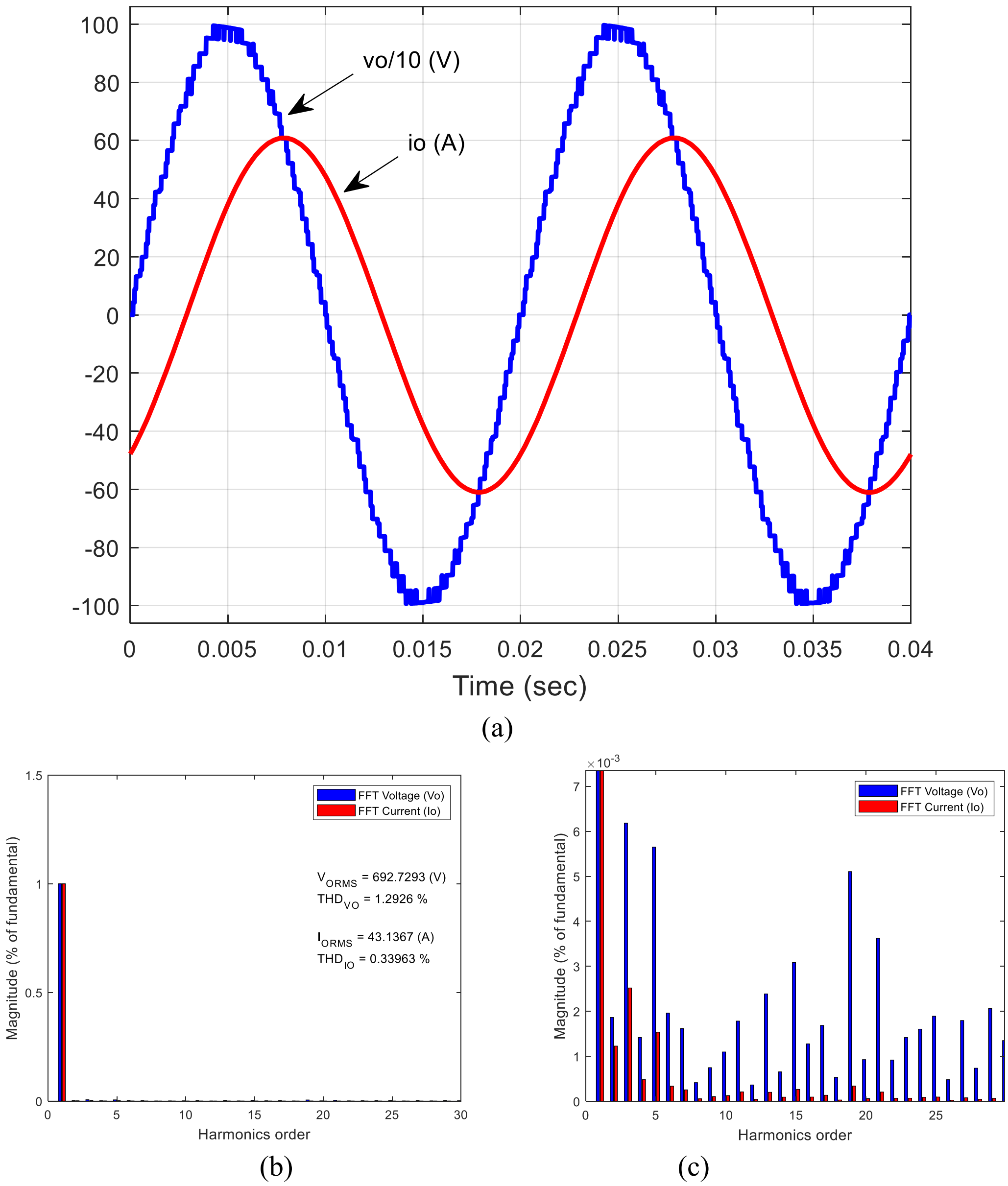

Fig. 21. Simulation results of the 49-level fed by PVs (a) output phase voltage and current with its (b) spectrum analyzer and (c) zoom section for the low harmonics order.

Table 4
Comparison of the three cases.

Case	Voltage Levels (V)	Power Factor (PF)	THDvo (%)	THDio (%)	Key Observations
Case 1	Per-unit system (1:2:7:14)	0.62	0.71216	0.093319	Uses a normalized voltage system, resulting in the lowest THDio.
Case 2	Actual voltages (40:80:280:560)	0.94	0.71227	0.16719	Higher PF compared to other cases, with slightly increased THDio.
Case 3	PV-boost output (40:80:280:560)	0.62	1.2926	0.33963	Replacing batteries with PVs significantly increases both THDvo and THDio.

The complete simulation results of the designed 49-level inverters with 12 switches show that the power quality resulting is within IEEE standards.

Table 5
Comparison of 49-level circuit with related MI topologies.

Ref.	Levels	No. of Switches	No. of Diodes	Input Sources	THDv	THDc
[19]	21	10	0	PV-BESS system	1.8 %	0.4 %
[22]	13	9	0	PV system	1.7 %	0.35 %
[26]	9	8	0	PV system	1.4 %	0.3 %
[27]	11	9	0	Solar photovoltaic system with UPFC	1.8 %	0.35 %
[28]	7	5	0	Renewable energy sources	2.7 %	0.65 %
[34]	5	12	–	PV system	4.3 %	2.4 %
[35]	7	14	–	PV system	3.4 %	2.1 %
Proposed Circuit	49	12	–	DC Battery (1:2:7:14) volt per unit system	0.7121 %	0.0933 %
Proposed Circuit	49	12	–	DC Battery (40:80:280:560) Actual voltage system	0.7122 %	0.1672 %
Proposed Circuit	49	12	–	PVs System (40:80:280:560) volt	1.2926 %	0.3396 %

5. Conclusion

The proposed policy of asymmetrical 49-levels cascaded inverter shows remarkable enhancement in mitigating the issues of power quality and harmonic distortion using DC sources and renewable power systems. This evaluation shows the ability of the inverter to provide low distortion, high quality sinusoidal waveforms under three scenarios. All these cases considered the effectiveness of the suggested power circuit and controller and provide good harmonic performance and waveform quality. In case 3, the PV sources give slightly worse THD compare to the other two cases but the overall results are still within the acceptable range proving the inverter's compatibility with green energy standalone systems. The proposed MLI with both DC sources and PV sources as inputs make it recommendable for various renewable energy applications. The system is working at different levels that makes it scalable and cost effective to generate 49 levels by using 12 switches with low THD. Due to laboratory availability restrictions, the primary approach focuses on analyzing performance through simulated methods for the designed inverter. Hardware implementation is recognized as crucial, and experimental validation is planned for future research. Future works can be done to develop the design MLI under various load conditions and controllers.

CRediT authorship contribution statement

Reving Masoud Abdulhakeem: Writing – original draft, Visualization, Software, Methodology, Data curation, Conceptualization. **Ali Kircay:** Writing – review & editing, Supervision, Resources. **Rakan Khalil Antar:** Writing – review & editing, Supervision, Methodology.

Declaration of competing interest

The authors declare that they have no known conflict of interest regarding the publication of this article. This research was conducted independently without any financial support or commercial affiliation that could influence the results or interpretations of this study. The study presents the design, analysis, and simulation of an asymmetrical 49-level inverter for renewable energy applications, with a focus on its performance under varying energy sources such as battery and photovoltaic (PV) modules. The authors affirm that the findings are based solely on the results of the simulations conducted and that no external parties have had any role in the study's design or interpretation.

Data availability

The authors do not have permission to share data.

References

[1] Jaber Fallah Ardashir, Mahya Hasannezhad, Hadi Vatankhah Ghadim, Sarhangzadeh Mitra, 13 - integration of energy storage systems with multilevel inverters for microgrids, in: Sivaraman Palanisamy, Sharmeela Chenniappan, Sanjeevikumar Padmanaban (Eds.), Distributed Energy Storage Systems for Digital Power Systems, Elsevier, 2025, pp. 293–318, https://doi.org/10.1016/B978-0-443-22013-5.00012-5. ISBN 9780443220135.
[2] Soumya Ranjan Das, Prakash K. Ray, A.K. Sahoo, Gaurav Dhiman, Application of optimisation technique in PV integrated multilevel inverter for power quality improvement, Comput. Electr. Eng. 97 (2022) 107606, https://doi.org/10.1016/j.compeleceng.2021.107606. ISSN 0045-7906.
[3] Hosseini Ehsan, Pablo Horrillo-Quintero, David Carrasco-Gonzalez, Pablo García-Triviño, Raúl Sarrias-Mena, Carlos A. García-Vázquez, Luis M. Fernández-Ramírez, Optimal energy management system for grid-connected hybrid power plant and battery integrated into multilevel configuration, Energy 294 (2024) 130765, https://doi.org/10.1016/j.energy.2024.130765. ISSN 0360-5442.
[4] C.R. Rajesh, P. Meenalochini, Sathish Kumar Kannaiah, A. Bindu, A hybrid control topology for cascaded H-bridge multilevel inverter to improve the power quality of smart grid connected system: NBO-RERNN approach, Expert Syst. Appl. 238 (Part C) (2024) 122054, https://doi.org/10.1016/j.eswa.2023.122054. ISSN 0957-4174.
[5] Fatiha Bouhadji, Ismail Bouyakoub, Fayçal Mehedi, Walid Mohammed Kacemi, Zakaria Reguieg, Optimization of grid power quality using third order sliding mode controller in PV systems with multilevel inverter, Energy Rep. 12 (2024) 5177–5193, https://doi.org/10.1016/j.egyr.2024.10.064. ISSN 2352-4847.
[6] Ashutosh Kumar Singh, Rajib Kumar Mandal, Switched-capacitor-based five-level inverter with closed-loop control for grid-connected PV application, Comput. Electr. Eng. 108 (2023) 108686, https://doi.org/10.1016/j.compeleceng.2023.108686. ISSN 0045-7906.
[7] G. Sathish Kumar, M. Krishna Paramathma, Optimal design of PV-SMES systems for power quality enhancement using pelicon optimized multi-level inverter model, Comput. Electr. Eng. 118 (Part B) (2024) 109404, https://doi.org/10.1016/j.compeleceng.2024.109404. ISSN 0045-7906.

[8] Kumari Akanksha, Yatindra Gopal, Dheeraj Kumar Dhaked, Kaibalya Prasad Panda, Y.N. Vijaya Kumar, A single source five-level switched-capacitor based multilevel inverter with reduced device count, e-Prime - advances in Electrical Engineering, Electronics and Energy 5 (2023) 100235, https://doi.org/10.1016/j.prime.2023.100235. ISSN 2772-6711.
[9] Shivinder Mehta, Vinod Puri, A review of different multi-level inverter topologies for grid integration of solar photovoltaic system, Renewable Energy Focus 43 (2022) 263–276, https://doi.org/10.1016/j.ref.2022.10.002. ISSN 1755-0084.
[10] Praveen Bansal, Shishir Dixit, Saket Gupta, Majed A. Alotaibi, Hasmat Malik, Fausto Pedro García Márquez, A robust modified notch filter based SOGI-PLL approach to control multilevel inverter under distorted grid, Ain Shams Eng. J. 15 (5) (2024) 102675, https://doi.org/10.1016/j.asej.2024.102675. ISSN 2090-4479.
[11] Fatima Chakir, Abdelmounime El Magri, Mohamed Kissaoui, Rachid Lajouad, Abderrahim El Fadili, Mostafa Chakir, Advanced control strategies for multilevel inverter in grid-connected and off-grid photovoltaic systems: a multi-objective approach using LS-PWM for THD reduction, Scientific African 26 (2024) e02472, https://doi.org/10.1016/j.sciaf.2024.e02472. ISSN 2468-2276.
[12] S. Jayaprakash, R. Balamurugan, S. Gopinath, T. Kokilavani, S. Maheswaran, 3-Phase multi-inverter with cascaded H-bridge inverter designing and implementation for renewable system, Sustain. Energy Technol. Assessments 52 (Part B) (2022) 102088, https://doi.org/10.1016/j.seta.2022.102088. ISSN 2213-1388.
[13] Younes El Khlifi, Abdelmounime El Magri, Rachid Lajouad, Omar Bouattane, Fouad Giri, Output-feedback control of a grid-connected photovoltaic system based on a multilevel flying-capacitor inverter with power smoothing capability, ISA (Instrum. Soc. Am.) Trans. 147 (2024) 360–381, https://doi.org/10.1016/j.isatra.2024.02.007. ISSN 0019-0578.
[14] K. Arulkumar, D. Vijayakumar, K. Palanisamy, Modeling and control strategy of three phase neutral point clamped multilevel PV inverter connected to the grid, J. Build. Eng. 3 (2015) 195–202, https://doi.org/10.1016/j.jobe.2015.06.001. ISSN 2352-7102.
[15] Pablo Horrillo-Quintero, Pablo García-Triviño, Raúl Sarrias-Mena, Carlos A. García-Vázquez, Luis M. Fernández-Ramírez, Fault-tolerant control for a microgrid with PV systems and energy storage systems integrated into quasi-Z-source cascaded H-bridge multilevel inverter, Elec. Power Syst. Res. 226 (2024) 109938, https://doi.org/10.1016/j.epsr.2023.109938. ISSN 0378-7796.
[16] Pablo Horrillo-Quintero, Pablo García-Triviño, Raúl Sarrias-Mena, Carlos A. García-Vázquez, Luis M. Fernández-Ramírez, Model predictive control of a microgrid with energy-stored quasi-Z-source cascaded H-bridge multilevel inverter and PV systems, Appl. Energy 346 (2023) 121390, https://doi.org/10.1016/j.apenergy.2023.121390. ISSN 0306-2619.
[17] G. Anusha, Krishan Arora, Himanshu Sharma, Surya Prakash Thota, Gyanendra Prasad Joshi, Woong Cho, Control strategies of 15-level modified cascaded H-bridge MLI with solar PV and energy storage system, Energy Rep. 12 (2024) 2–26, https://doi.org/10.1016/j.egyr.2024.06.003. ISSN 2352-4847.
[18] F. Chakir, A. El Magri, R. Lajouad, M. Kissaoui, M. Chakir, O. Bouattan, Enhanced standalone photovoltaic system with novel multi-level inverter and nonlinear control for improved THD and converter efficiency, IFAC-PapersOnLine 58 (13) (2024) 478–483, https://doi.org/10.1016/j.ifacol.2024.07.528. ISSN 2405-8963.
[19] Pasquale Franzese, Mattia Ribera, Andrea Cervone, Diego Iannuzzi, Optimized control strategy for single-phase multilevel cascaded converter in a distributed PV-BESS system, Elec. Power Syst. Res. 214 (Part A) (2023) 108818, https://doi.org/10.1016/j.epsr.2022.108818. ISSN 0378-7796.
[20] S. Narendiran, Sarat Kumar Sahoo, A single phase reduced device count multilevel inverter topology using MCPWM for renewable energy systems, Energy Proc. 117 (2017) 244–251, https://doi.org/10.1016/j.egypro.2017.05.128. ISSN 1876-6102.
[21] Darvish Falehi Ali, Novel chattering free binomial hyperbolic sliding mode controller for asymmetric cascaded E-type bonded T-type multilevel inverter-based dynamic voltage restorer to meliorate FRT capability of DFIG-based wind turbine, Results in Engineering 23 (2024) 102370, https://doi.org/10.1016/j.rineng.2024.102370. ISSN 2590-1230.
[22] Sambasivam Rajalakshmi, Dr Parthasarathy Rangarajan, Investigation of modified multilevel inverter topology for PV system, Microprocess. Microsyst. 71 (2019) 102870, https://doi.org/10.1016/j.micpro.2019.102870. ISSN 0141-9331.
[23] Soumya Ranjan Das, Arun Kumar Sahoo, Gaurav Dhiman, Krishna Kant Singh, Akansha Singh, Photo voltaic integrated multilevel inverter based hybrid filter using spotted hyena optimizer, Comput. Electr. Eng. 96 (Part A) (2021) 107510, https://doi.org/10.1016/j.compeleceng.2021.107510. ISSN 0045-7906.
[24] Hakki Mollahasanoglu, Merve Mollahasanoglu, Emre Ozkop, Comparative study of single-phase multilevel cascaded transformerless inverters with different modulation methods, Engineering Science and Technology, an International Journal 51 (2024) 101652, https://doi.org/10.1016/j.jestch.2024.101652. ISSN 2215-0986.
[25] Panagiotis Kakosimos, Konstantinos Pavlou, Antonios Kladas, Stefanos Manias, A single-phase nine-level inverter for renewable energy systems employing model predictive control, Energy Convers. Manag. 89 (2015) 427–437, https://doi.org/10.1016/j.enconman.2014.10.013. ISSN 0196-8904.
[26] N. Prabaharan, A. Rini Ann Jerin, K. Palanisamy, S. Umashankar, Integration of single phase reduced switch multilevel inverter topology for grid connected photovoltaic system, Energy Proc. 138 (2017) 1177–1183, https://doi.org/10.1016/j.egypro.2017.10.231. ISSN 1876-6102.
[27] Swetha Monica, Alok Kumar Singh, D. Vijaya Kumar, An RFCSO-based grid stability enhancement by integrating solar photovoltaic systems with multilevel unified power flow controllers, Energy Storage and Saving (2024), https://doi.org/10.1016/j.enss.2024.10.004. ISSN 2772-6835.
[28] Nallam Vani Annapurna Bhavani, Alok Kumar Singh, D. Vijaya Kumar, Optimized integration of renewable energy sources using seven-level converter controlled by ANFIS-CS-GWO, e-Prime - advances in Electrical Engineering, Electronics and Energy 9 (2024) 100689, https://doi.org/10.1016/j.prime.2024.100689. ISSN 2772-6711.
[29] Y.V. Pavan Kumar, Bhimasingu Ravikumar, A simple modular multilevel inverter topology for the power quality improvement in renewable energy based green building microgrids, Elec. Power Syst. Res. 140 (2016) 147–161, https://doi.org/10.1016/j.epsr.2016.06.027. ISSN 0378-7796.
[30] Bhupender Sharma, Ratna Dahiya, Jayaram Nakka, Effective grid connected power injection scheme using multilevel inverter-based hybrid wind solar energy conversion system, Elec. Power Syst. Res. 171 (2019) 1–14, https://doi.org/10.1016/j.epsr.2019.01.044. ISSN 0378-7796.
[31] Hossien Faraji, Amir Khorsandi, Seyed Hossein Hosseinian, Multi-level coordinated control of islanded DC microgrid integrated with electric vehicle charging stations with fault ride-through capability, J. Clean. Prod. 420 (2023) 138372, https://doi.org/10.1016/j.jclepro.2023.138372. ISSN 0959-6526.
[32] R.K. Antar, Design a multilevel inverter circuit based on different control structures, International Journal of Advanced Technology and Engineering Exploration 11 (115) (2024) 943.
[33] R.M. Abdulhakeem, A. Kircay, R.K. Antar, Renewable power energy management for single and three-phase inverters design, Energy Rep. 12 (2024) 3096–3113.
[34] T. Tarmizi, S. Taib, M.K. Desa, Design and verification of improved cascaded multilevel inverter topology with asymmetric dc sources, Journal of Power Electronics 19 (5) (2019) 1074–1086.
[35] R. Sen Goopta, A. Bhattacharya, Asymmetrically switched CHB multilevel inverters with harmonic mitigation techniques applied to photovoltaic power generation, IETE J. Res. 68 (6) (2022) 4360–4382.
[36] K. Vanchinathan, K.R. Valluvan, C. Gnanavel, C. Gokul, Numerical simulation and experimental verification of fractional-order PI^{λ} controller for solar PV fed sensorless brushless DC motor using whale optimization algorithm, Elec. Power Compon. Syst. 50 (1–2) (2022) 64–80, https://doi.org/10.1080/15325008.2022.2135644.
[37] K. Vanchinathan, K.R. Valluvan, C. Gnanavel, C. Gokul, Design methodology and experimental verification of intelligent speed controllers for sensorless permanent magnet Brushless DC motor, International Transactions on Electrical Energy Systems 31 (9) (2021), https://doi.org/10.1002/2050-7038.12991.
[38] K. Vanchinathan, N. Selvaganesan, Adaptive fractional order PID controller tuning for brushless DC motor using Artificial Bee Colony algorithm, Results in Control and Optimization 4 (2021) 100032, https://doi.org/10.1016/j.rico.2021.100032.
[39] K. Vanchinathan, K.R. Valluvan, A metaheuristic Optimization approach for tuning of Fractional-Order PID controller for speed control of sensorless BLDC motor, J. Circ. Syst. Comput. 27 (8) (2017) 1850123, https://doi.org/10.1142/s0218126618501232.
[40] R.K. Antar, Design a multilevel inverter circuit based on different control structures, International Journal of Advanced Technology and Engineering Exploration 11 (115) (2024) 943–954, https://doi.org/10.19101/IJATEE.2024.111100040.